

REPORT DOCUMENTATION PAGE				Form Approved OMB No. 0704-0188	
Public reporting burden for this collection of information is estimated to average 1 hour per response, including the time for reviewing instructions, searching existing data sources, gathering and maintaining the data needed, and completing and reviewing this collection of information. Send comments regarding this burden estimate or any other aspect of this collection of information, including suggestions for reducing this burden to Department of Defense, Washington Headquarters Services, Directorate for Information Operations and Reports (0704-0188), 1215 Jefferson Davis Highway, Suite 1204, Arlington, VA 22202-4302. Respondents should be aware that notwithstanding any other provision of law, no person shall be subject to any penalty for failing to comply with a collection of information if it does not display a currently valid OMB control number. PLEASE DO NOT RETURN YOUR FORM TO THE ABOVE ADDRESS.					
1. REPORT DATE (DD-MM-YYYY) Mar 2014		2. REPORT TYPE Briefing Charts		3. DATES COVERED (From - To) Mar 2014- May 2014	
4. TITLE AND SUBTITLE High Temperature Latent Heat Thermal Energy Storage to Augment Solar Thermal Propulsion for Microsats				5a. CONTRACT NUMBER In-House	
				5b. GRANT NUMBER	
				5c. PROGRAM ELEMENT NUMBER	
6. AUTHOR(S) Matthew R. Gilpin, David B. Scharfe, Marcus P. Young, Rebecca N. Webb				5d. PROJECT NUMBER	
				5e. TASK NUMBER	
				5f. WORK UNIT NUMBER Q0CA	
7. PERFORMING ORGANIZATION NAME(S) AND ADDRESS(ES) Air Force Research Laboratory (AFMC) AFRL/RQRS 1 Ara Drive. Edwards AFB CA 93524-7013				8. PERFORMING ORGANIZATION REPORT NO.	
9. SPONSORING / MONITORING AGENCY NAME(S) AND ADDRESS(ES) Air Force Research Laboratory (AFMC) AFRL/RQR 5 Pollux Drive. Edwards AFB CA 93524-7048				10. SPONSOR/MONITOR'S ACRONYM(S)	
				11. SPONSOR/MONITOR'S REPORT NUMBER(S) AFRL-RQ-ED-VG-2014-075	
12. DISTRIBUTION / AVAILABILITY STATEMENT Distribution A: Approved for Public Release; Distribution Unlimited					
13. SUPPLEMENTARY NOTES Briefing Charts presented at 11th Annual AIAA Southern California Aerospace Systems and Technology Conference, Santa Ana, CA, May 3rd, 2014. PA#14162					
14. ABSTRACT Briefing Charts					
15. SUBJECT TERMS					
16. SECURITY CLASSIFICATION OF:			17. LIMITATION OF ABSTRACT SAR	18. NUMBER OF PAGES 65	19a. NAME OF RESPONSIBLE PERSON Marcus Young
a. REPORT Unclassified	b. ABSTRACT Unclassified	c. THIS PAGE Unclassified			19b. TELEPHONE NO (include area code) 661-275-6264

High Temperature Latent Heat Thermal Energy Storage to Augment Solar Thermal Propulsion for Microsatellites

Matthew R. Gilpin, USC

David B. Scharfe, ERC, Inc.

Marcus P. Young, ARFL/RQRS

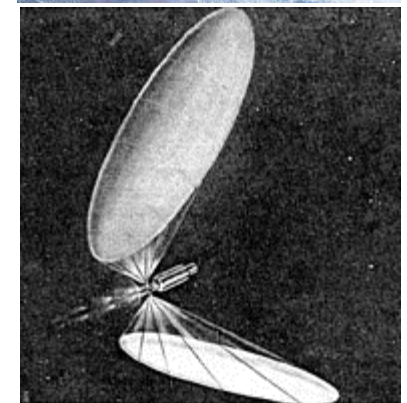
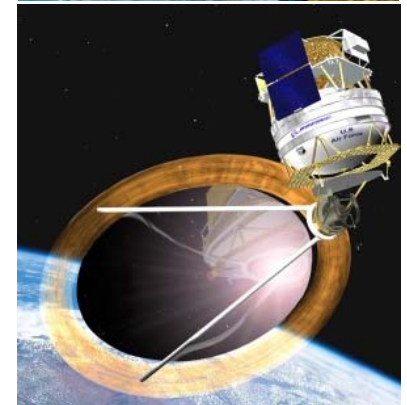
Rebecca N. Webb, UCCS

AFRL

THE AIR FORCE RESEARCH LABORATORY
LEAD | DISCOVER | DEVELOP | DELIVER

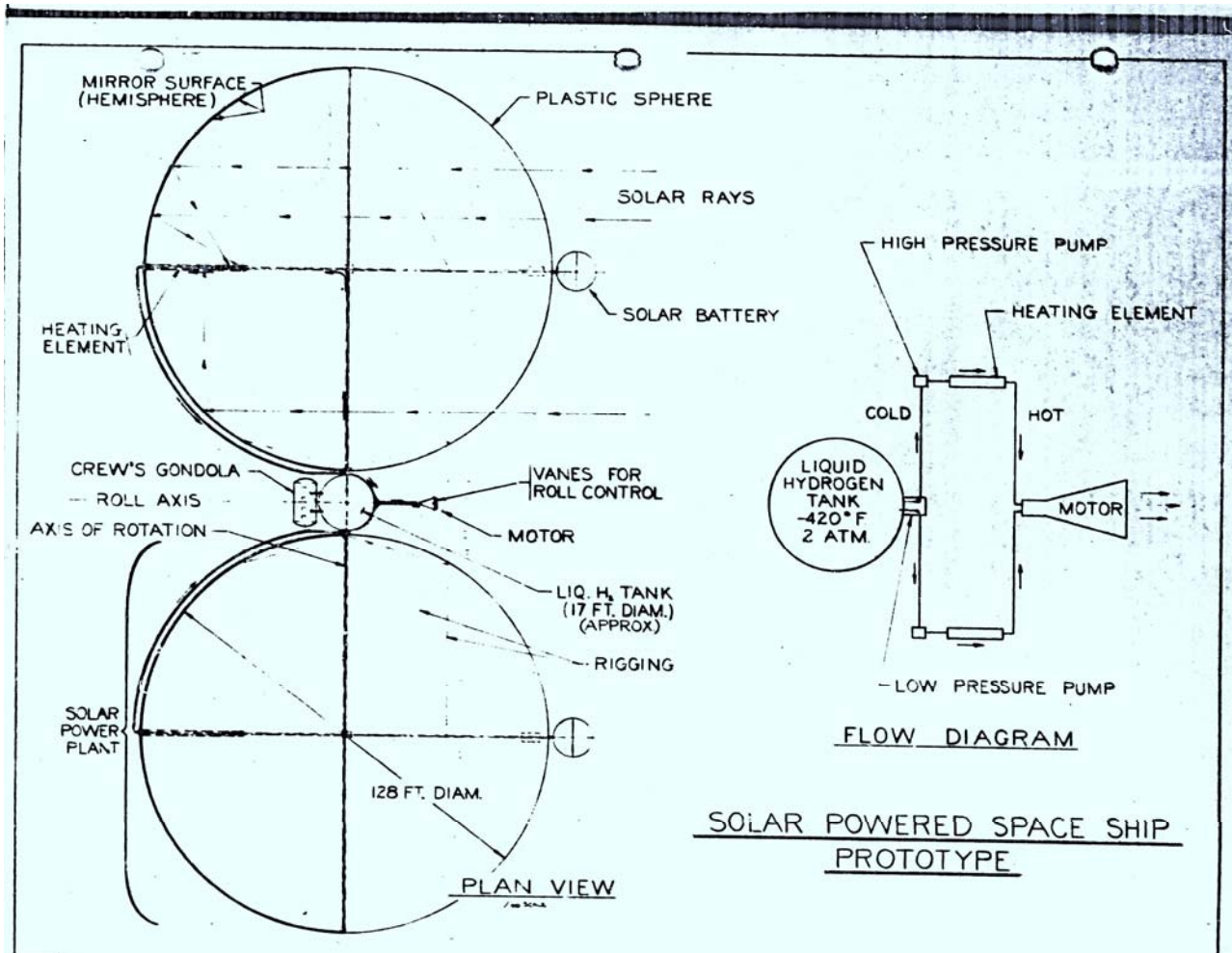
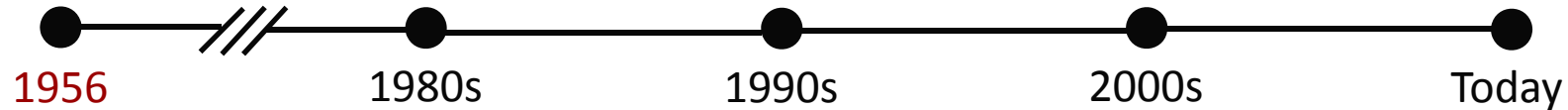


- Solar thermal propulsion (STP) has over 50 years of developmental history and offers a compromise between thrust and efficiency
- No solar thermal spacecraft have been flown
 - Complicated architecture
 - System scale
 - Adverse mission impact
- It is proposed here that a bi-modal solar thermal microsatellite has the potential to greatly increase the operating envelope of the platform
- The development of **high temperature latent heat thermal energy storage** is currently an enabling technology

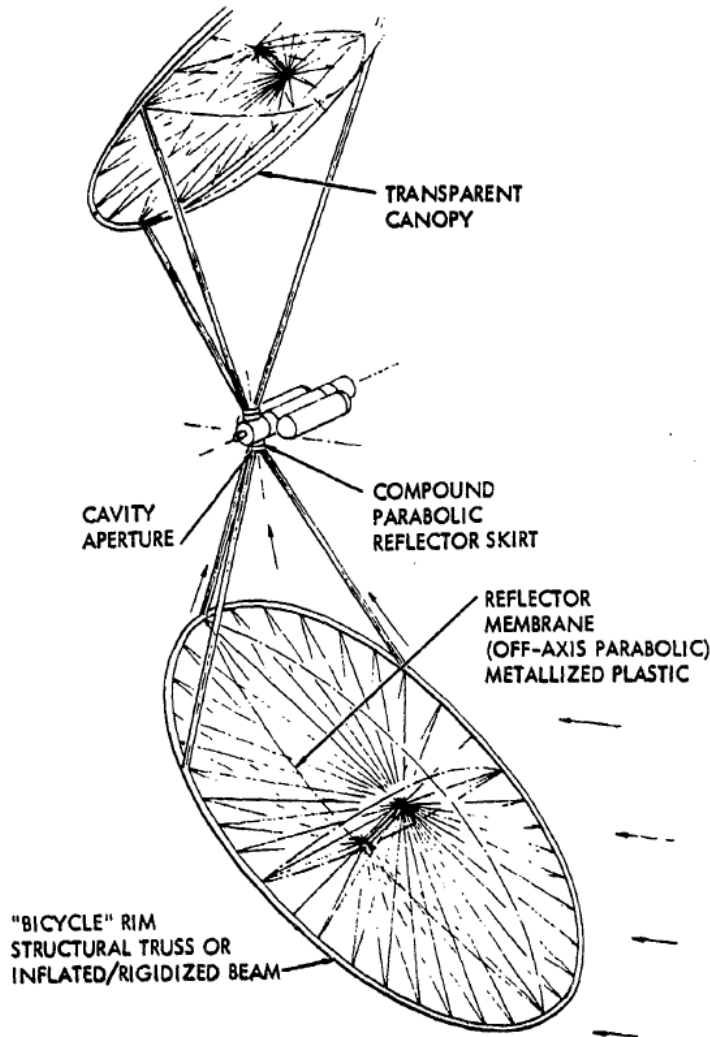
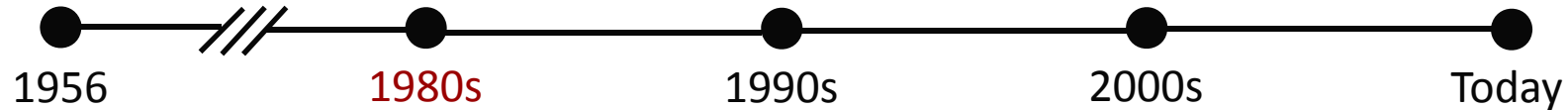




1. Solar Thermal Propulsion Overview
 - Technological History
 - Developmental Milestones
2. Bi-modal Solar Thermal Microsatellite
 - Technological Requirements
 - Phase Change Material Selection
 - Performance Evaluation
3. Proposed Study
4. Current Work / Results
 - USC Solar Furnace
 - Materials Studies
 - Modeling Capability
 - Experimental Results
5. Future Work & Project Conclusions

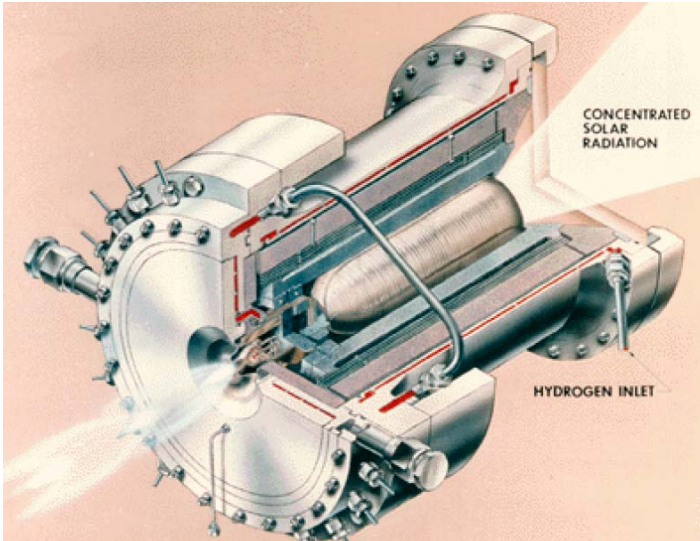
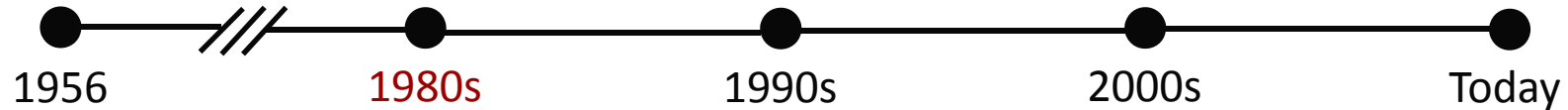


- “Solar Powered Space Ship” proposed by Krafft Ehricke
- 7500 kg spacecraft with a two man crew
- AFRPL funded investigation at Electro-Optical Systems (EOS) in 1963 produced solar heated H₂ at approx. 2300 K
- Work halted due to concerns about “awkward” vehicle design and integration issues
- Funding was shifted to a competing advanced concept



- Space Shuttle – “represents a national commitment to extended operations in space” *Selph 1981*
- 1979 Rockwell report, funded through AFRPL, concludes a solar thermal rocket is possible and recommends near term production
- Vehicle integration was greatly simplified by a centrally located solar receiver and inflatable concentrators
- Compared performance of **28,100 kg**, shuttle launched spacecraft for LEO-GEO transfer

Engine Type	LO ₂ -H ₂	Ion	Solar 1	Solar 2
ΔV (m/s)	4,270	5,850	5,850	4,800
Isp (sec)	475	2,940	872	872
Trip Time (days)	5	180	14	40
Payload to Geo (kg)	9,250	20,000	9,300	13,200



- AFRPL funded effort for experimental demonstration based on findings of Rockwell report
- Rocketdyne contracted to produce a solar thermal thruster using coiled rhenium tubing with a target exit temperature of 2705 K
- Solar furnace problems limited testing temperatures to approximately 1800 K
- AFRPL declared technology “feasible” but development was slowed in 1989 due to budget cut-backs
- Note that the design **does not** include a means of thermal energy storage

“...time spent traversing the Earth shadow results in a trip-time increase of approximately 10% at no increase in propellant expended.”

Ethridge 1979



- A **bi-modal** nuclear thermal system capable of providing propulsive and electrical power was proposed in the early 1990s
- Integrated upper stage design supplies electrical power to the payload after orbit transfer
- Reduced mass: potential for launch vehicle “step down”

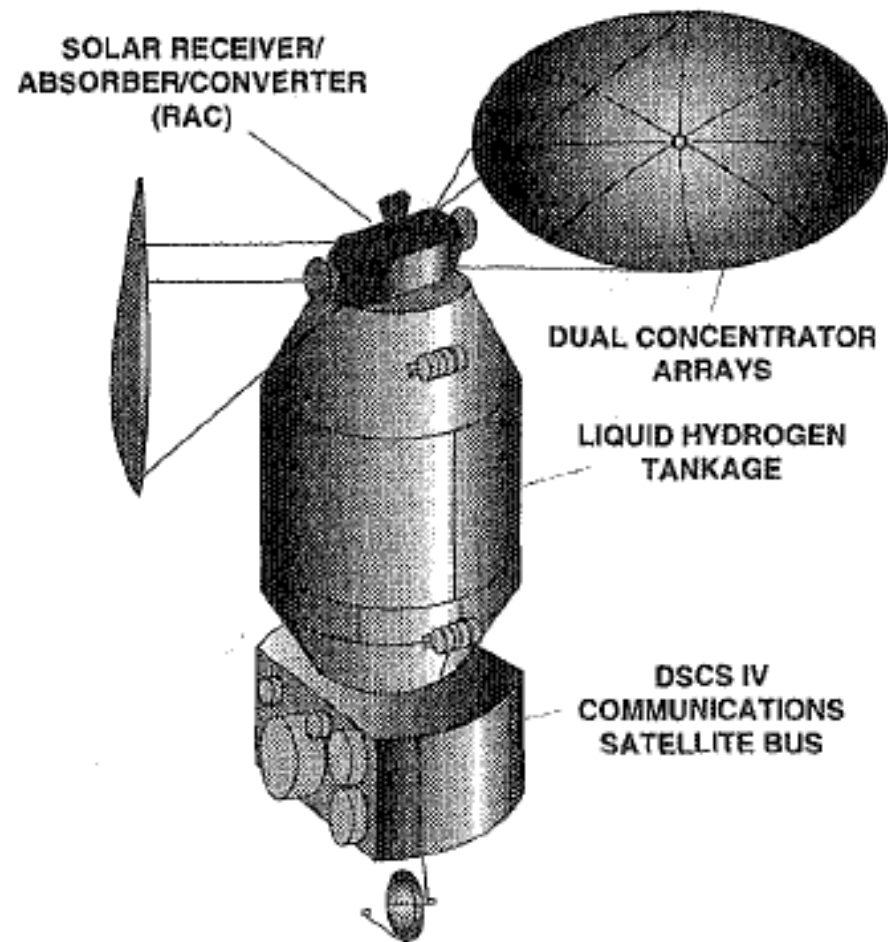
Delta II 7925

\$50M in 1995
1800 kg to GTO

Titan IIG

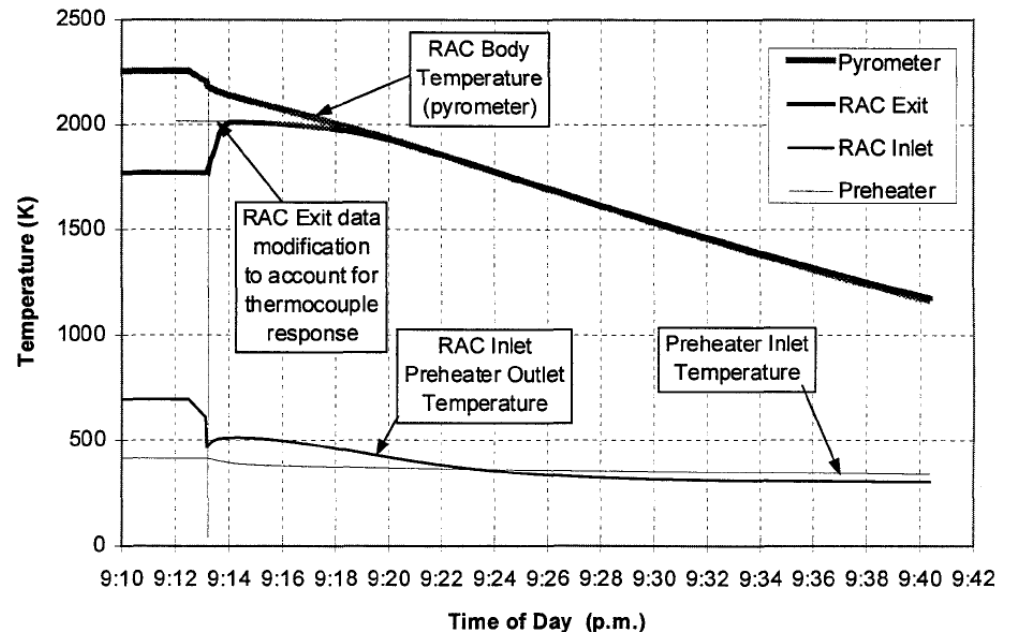
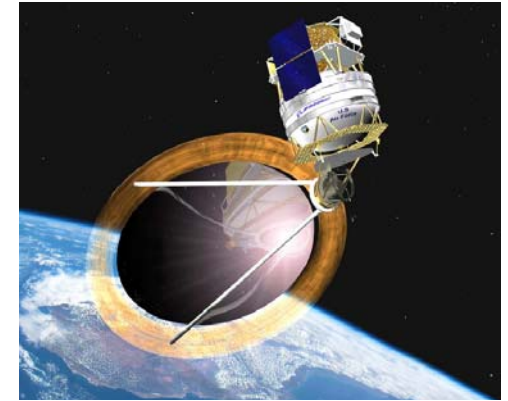
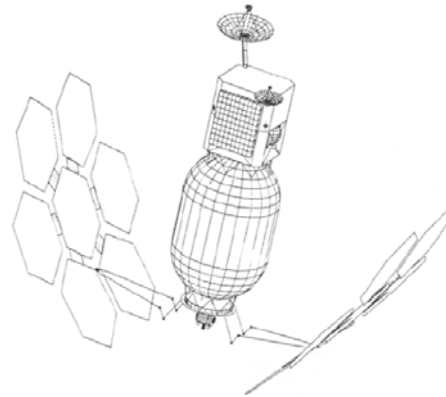
\$18-30M in 1995
1000 kg to GTO

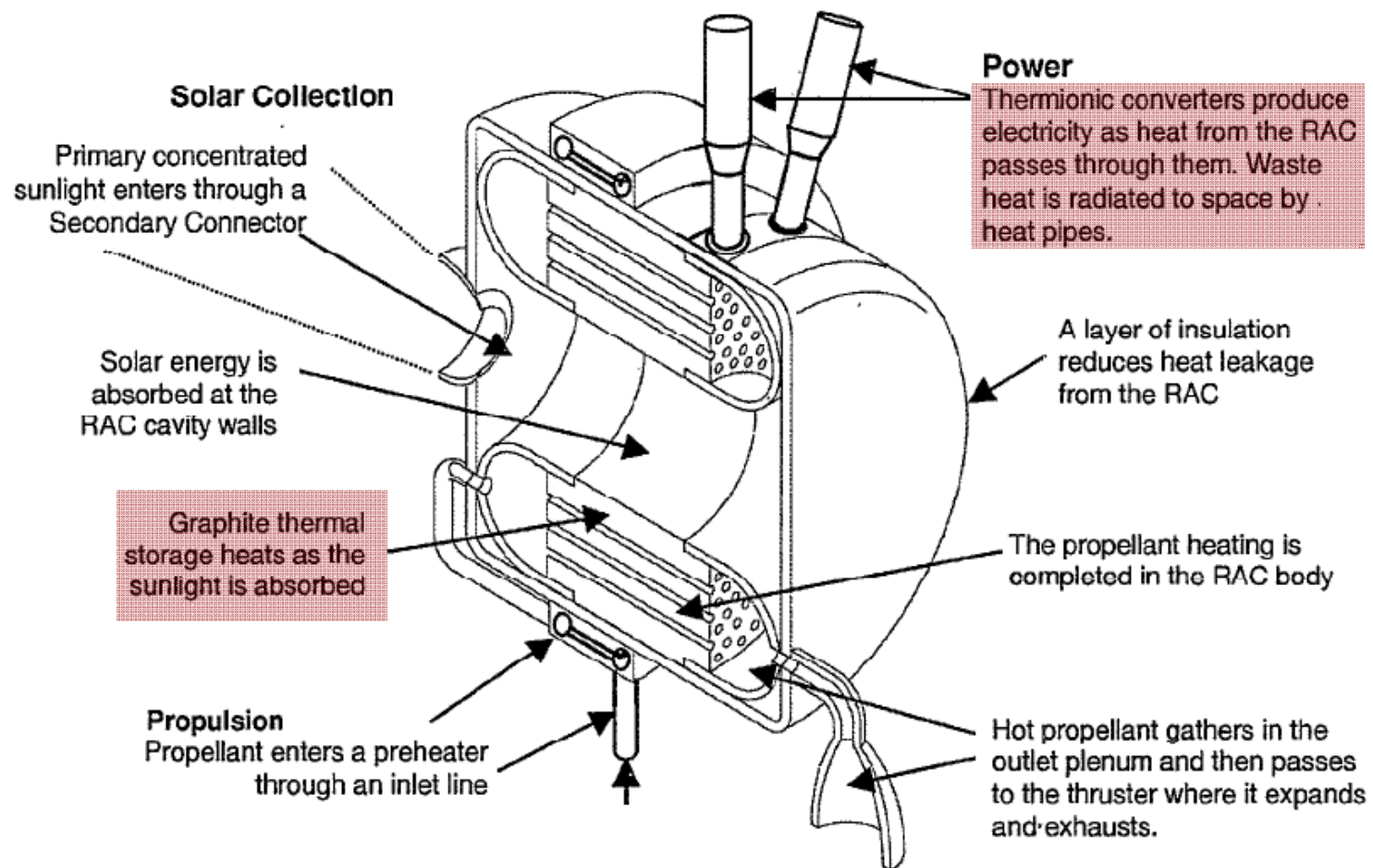
- Due to waning interest in nuclear thermal research, AFRPL considered the concept with a solar thermal architecture
- Sought to quickly reduce the cost of Air Force space operations using *existing* technology

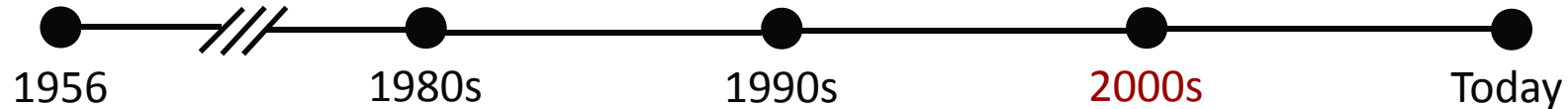




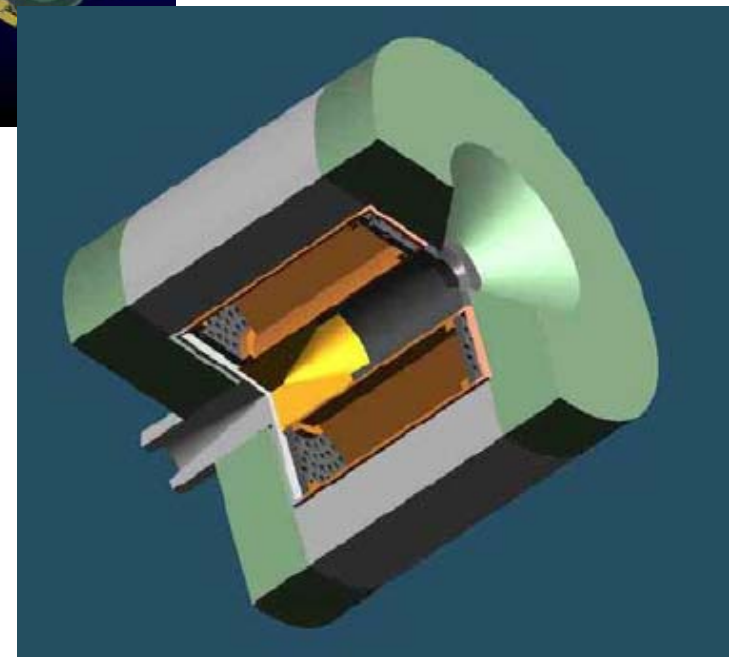
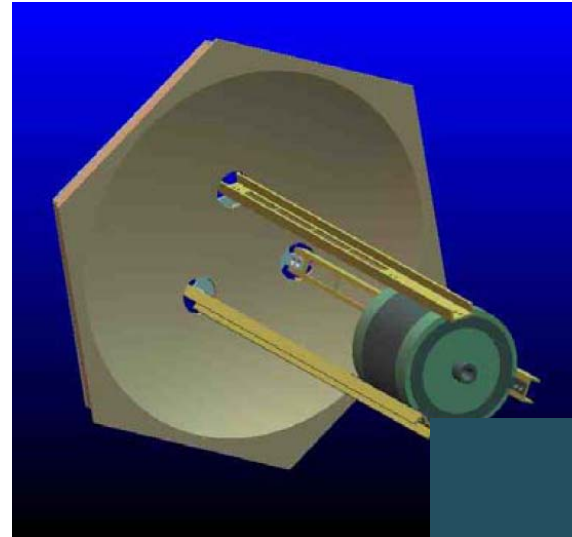
- Integrated Solar Upper Stage Program (ISUS) initiated in 1994
- ISUS program targeted a “militarily” useful payload on orbit by 1998 – *very optimistic*
- Performed a ground test of a prototype Receiver-Absorber-Converter (RAC)
- RAC incorporated sensible heat thermal energy storage – necessitated by the bi-modal design
- Succeeded in recording data for hot flow hydrogen testing
- Program closed in 1998 – followed by Boeing Solar Orbit Transfer Vehicle (SOTV) and the STP Critical Flight Experiment at NASA Marshall

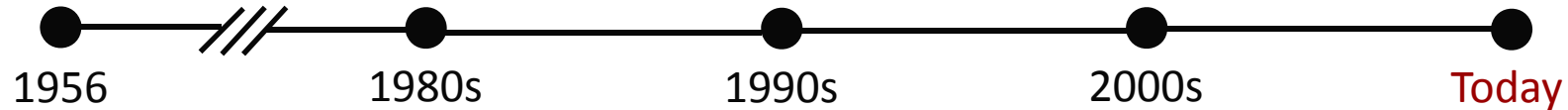






- Concept shifted to microsatellites (10-100 kg) in an effort to *finally* mount a space demonstration
- Project headed by Kennedy, a veteran of the ISUS program, at Surrey Space Center
- Proposed the use of non-cryogenic propellants such as N_2H_4 and NH_3 and “packed bed” sensible heat thermal energy storage
- Achieved experimental NH_3 temperatures approaching 2000 K
- Other small scale research efforts
 - Thin film concentrator and Mo receiver work at JAXA
 - Fiber optic coupling work at Physical Sciences Inc



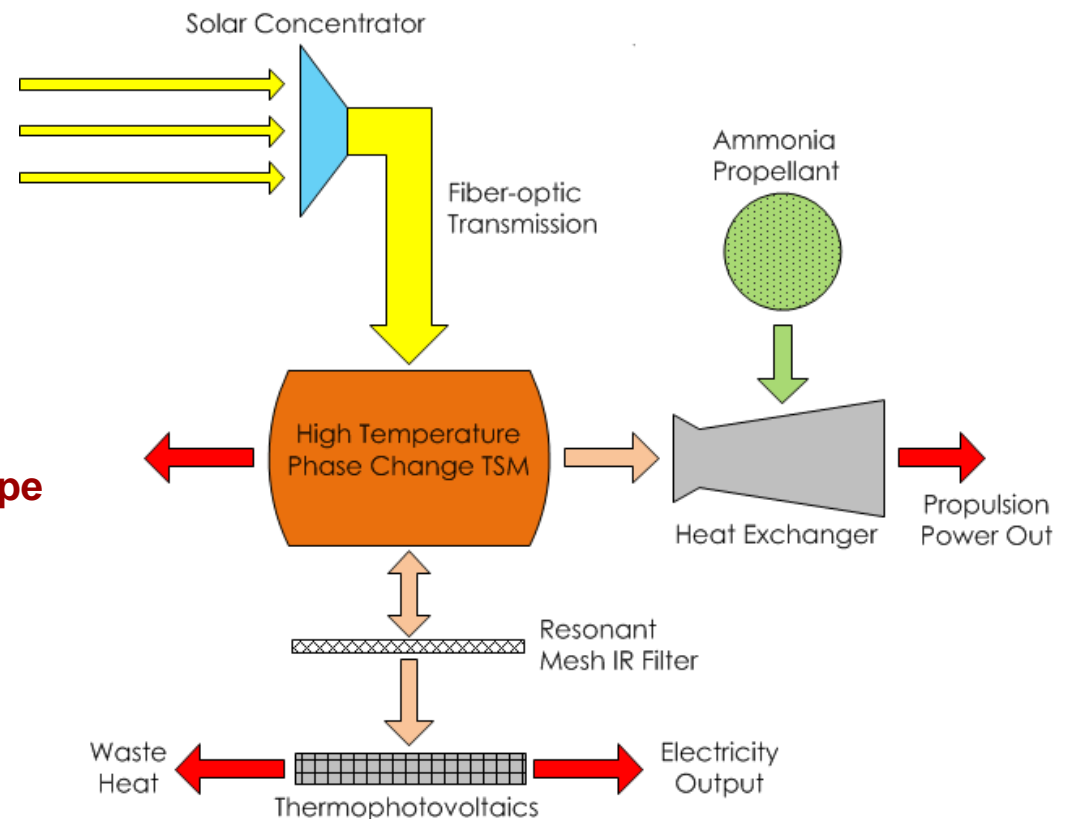


- Drawing from Kennedy's microsatellite study, a review by the AFRL advanced concepts group identified STP as a promising candidate for high performance microsatellite missions
- A **bi-modal microsatellite** configuration is proposed and further study is recommended
- Microsatellite scaling distinguishes STP
- Large ΔV (> 1 km/s) possible

Expand the Microsatellite Operating Envelope

- Expand possible "piggy-back" launch options
- GEO Insertion: ~ 1760 m/s
- Near Escape Missions: $\sim 770 - 1770$ m/s

Possible with EP, however, STP offers a much shorter burn time and higher maneuverability





☐ Solar Concentrators

- 10,000 :1 Concentration Ratio
- Low mass and deployable

☐ Fiber Optic Coupling

- High transmission efficiency
- High pointing accuracy

☐ Thermal-Electric Conversion

- Operational at high temperatures
- High specific power

☐ Advanced Insulation

- Low Mass
- High Temperature

☐ High Temperature Storage Material

- Matches STP propulsion temperatures
- High energy density ($> 1000+$ kJ/Kg)

☐ Compatible / Effective RAC

- Long term compatibility
- Effective energy coupling

☒ **Solar Concentrators**

- 10,000 :1 Concentration Ratio
- Low mass and deployable

☐ **Fiber Optic Coupling**

- High transmission efficiency
- High pointing accuracy

☐ **Thermal-Electric Conversion**

- Operational at high temperatures
- High specific power

☐ **Advanced Insulation**

- Low Mass
- High Temperature

☐ **High Temperature Storage Material**

- Matches STP propulsion temperatures
- High energy density ($> 1000+ \text{ kJ/Kg}$)

☐ **Compatible / Effective RAC**

- Long term compatibility
- Effective energy coupling

- Thin PMA (JAXA) “flight ready” concentrators achieve 200 g/m^2 and C. ratios $> 10,000:1$
- Inflatables (AFRL, SRS) can achieve $< 1 \text{ kg/m}^2$ and have been reported as being “optical quality”
- Large rigid structures (NASA SD, ISUS) are listed at approx. 3 kg/m^2 including mounting, tracking, and deployment
- Microsatellite scale system only requires $< 2 \text{ m}^2$



Sahara 2004



SRS Technologies

☒ Solar Concentrators

- 10,000 :1 Concentration Ratio
- Low mass and deployable

☒ Fiber Optic Coupling

- High transmission efficiency
- High pointing accuracy

☐ Thermal-Electric Conversion

- Operational at high temperatures
- High specific power

☐ Advanced Insulation

- Low Mass
- High Temperature

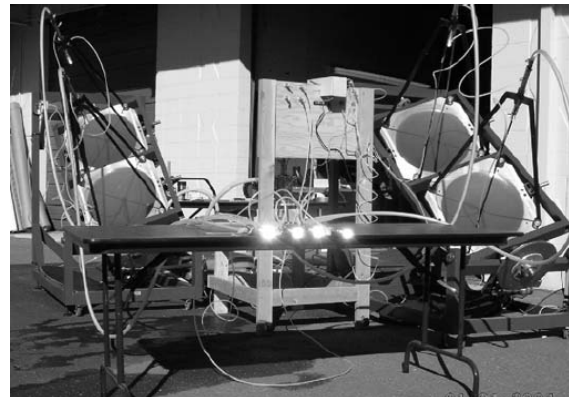
☐ High Temperature Storage Material

- Matches STP propulsion temperatures
- High energy density ($> 1000+ \text{ kJ/Kg}$)

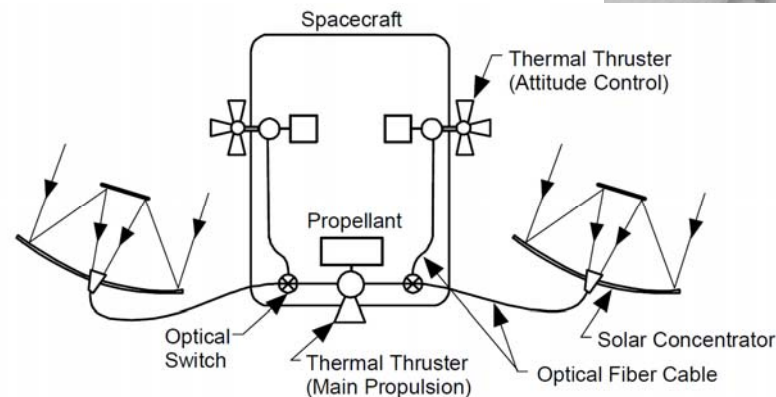
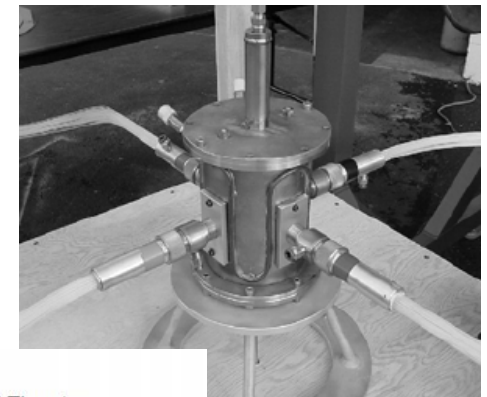
☐ Compatible / Effective RAC

- Long term compatibility
- Effective energy coupling

- Current lab systems operate at 35% η_{total}
- Estimated 70% η_{total} for a space qualified system from better materials selection
- Pointing accuracy of approx. 0.1° required



Nakamura 2004



☒ Solar Concentrators

- 10,000 :1 Concentration Ratio
- Low mass and deployable

☒ Fiber Optic Coupling

- High transmission efficiency
- High pointing accuracy

☒ Thermal-Electric Conversion

- Operational at high temperatures
- High specific power

☐ Advanced Insulation

- Low Mass
- High Temperature

☐ High Temperature Storage Material

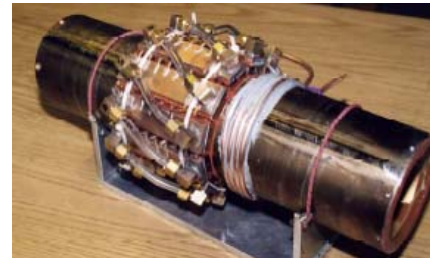
- Matches STP propulsion temperatures
- High energy density ($> 1000+$ kJ/Kg)

☐ Compatible / Effective RAC

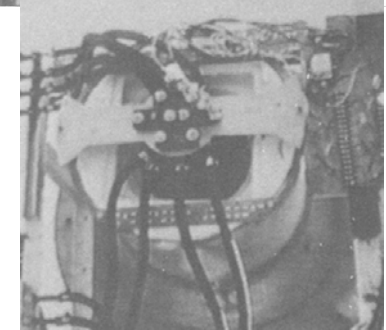
- Long term compatibility
- Effective energy coupling

- Thermophotovoltaics are the strongest candidate
- Operation targets properly matched to solar thermal temperatures.
- 15 W/kg in current systems, including radiator
- Closed Brayton and thermionics scale poorly for microsats

Edtek



McDonnell Douglas





☒ Solar Concentrators

- 10,000 :1 Concentration Ratio
- Low mass and deployable

☒ Fiber Optic Coupling

- High transmission efficiency
- High pointing accuracy

☒ Thermal-Electric Conversion

- Operational at high temperatures
- High specific power

☒ Advanced Insulation

- Low Mass
- High Temperature

☐ High Temperature Storage Material

- Matches STP propulsion temperatures
- High energy density (> 1000+ kJ/Kg)

☐ Compatible / Effective RAC

- Long term compatibility
- Effective energy coupling

Material	k_{th} @ 1000 C (W/mK)	k_{th} @ 1500 C (W/mK)	k_{th} @ 2000 C (W/mK)	Density (g/cm ³)
Silicon Carbide	45	30	25	3.2
Boron Nitride	17-33	22.5	18	1.8
Alumina	6.5	6.6	--	3.8
Zirconia	2	2.5	3	5.5
ONRL CBCF	0.17	0.2	0.26	0.2
Calcarb CBCF	0.2	0.35	0.65	0.18
Aerogel Filled Graphite Foams	0.25	0.4	0.75	0.07
Mo - ZrO ₂ Multifoil	0.001	0.05	0.1	1.4

- Must operate between **1500 – 2600 K**

• Carbon Bonded Carbon Fiber

- Can draw from NASA RTG development
- Carbon foams with filler to limit radiation loss currently offered by ULTRAMET

• Low Emissivity Vacuum Gap

- Typically the first stage in a TPV system
- Mo/ZrO₂ multifoil blankets also produced for RTGs

• Ceramic Doped Aerogels

- Underdevelopment with JPL, RZSM, and RQRS



☒ **Solar Concentrators**

- 10,000 :1 Concentration Ratio
- Low mass and deployable

☒ **Fiber Optic Coupling**

- High transmission efficiency
- High pointing accuracy

☒ **Thermal-Electric Conversion**

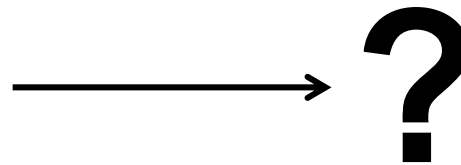
- Operational at high temperatures
- High specific power

☒ **Advanced Insulation**

- Low Mass
- High Temperature

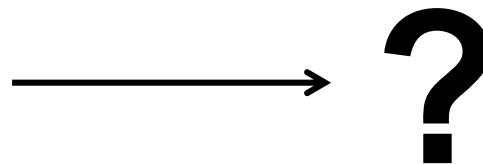
☐ **High Temperature Storage Material**

- Matches STP propulsion temperatures
- High energy density ($> 1000+$ kJ/Kg)



☐ **Compatible / Effective RAC**

- Long term compatibility
- Effective energy coupling



To date, all STP systems have used sensible heat thermal energy storage

Material	T_{melt} [K]	C_p @ 2500 K [kJ/kgK]	ΔT Required for 1 MJ/kg
Graphite	3923	2.15	475
Boron Carbide	2700	2.68	380
Silicon Carbide	2818	1.01	740
Boron Nitride	3273	1.98	510

- Simplified engineering suitable for time constrained development – Low TRL level of other options
- “...moderate yet acceptable performance” - Kennedy 2002



ISUS Data Analysis

- Seven minute “steady” burn corresponds to an “effective” energy storage density of **0.5 MJ/kg**
- When the RAC achieves 1 MJ/kg, **exit temp** has dropped by **> 25%** and **Isp** has dropped by **15%**
- ISUS spec for thermionic hot shoe temperature was 1900 – 2200 K. If allowed for a radiatively coupled TPV system, this would correspond to a **> 50% decrease** in power output

Terrestrial Phase Change Materials

Class	T_{melt} [K]	ΔH_{fus} [MJ/kg]	k_{th} [W/mK]
Paraffin Wax	317 – 379	0.072 – 0.214	0.19 – 0.75
Fatty Acids	268 – 344	0.045 – 0.210	0.14 – 0.17
Hydrated Salts	281 – 1170	0.115 – 0.492	0.46 – 5.0

- Energy density and k_{th} an order of magnitude too low
- Melt temperatures too slow for STP
- Decomposition after repeated cycling

Terrestrial Phase Change Materials

Class	T_{melt} [K]	ΔH_{fus} [MJ/kg]	k_{th} [W/mK]
Paraffin Wax	317 – 379	0.072 – 0.214	0.19 – 0.75
Fatty Acids	268 – 344	0.045 – 0.210	0.14 – 0.17
Hydrated Salts	281 – 1170	0.115 – 0.492	0.46 – 5.0

Potential High-Temp Phase Change Materials

Material	T_{melt} [K]	ΔH_{fus} [MJ/kg]	k_{th} @ T_{melt} [W/mK]
MgF ₂	1536	0.94	3.8
Beryllium	1560	1.31	69
Silicon	1687	1.79	20
Nickel	1728	0.3	83
Scandium	1814	0.31	16
Chromium	2180	0.4	48
Vanadium	2183	0.45	51
Boron	2350	4.6	10
Ruthenium	2607	0.38	80
Niobium	2750	0.29	82
Molybdenum	2896	375	84

Terrestrial Phase Change Materials

Class	T_{melt} [K]	ΔH_{fus} [MJ/kg]	k_{th} [W/mK]
Paraffin Wax	317 – 379	0.072 – 0.214	0.19 – 0.75
Fatty Acids	268 – 344	0.045 – 0.210	0.14 – 0.17
Hydrated Salts	281 – 1170	0.115 – 0.492	0.46 – 5.0

Potential High-Temp Phase Change Materials

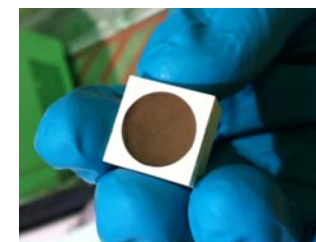
Material	T_{melt} [K]	ΔH_{fus} [MJ/kg]	k_{th} @ T_{melt} [W/mK]
MgF ₂	1536	0.94	3.8
Beryllium	1560	1.31	69
Silicon	1687	1.79	20
Nickel	1728	0.3	83
Scandium	1814	0.31	16
Chromium	2180	0.4	48
Vanadium	2183	0.45	51
Boron	2350	4.6	10
Ruthenium	2607	0.38	80
Niobium	2750	0.29	82
Molybdenum	2896	.38	84

Silicon



- Moderate Performance
- 330s I_{sp}

Boron



- High Performance
- 390s I_{sp}



Bi-Modal System Performance Parameters
100 kg Microsatellite - 100 W continuous power draw

Silicon System		
Thermal Collection	5.3	kg
Thermal Storage	3.3	kg
Power	6.7	kg
Propellant	36.7	kg
Tankage / Thruster	6.1	kg
Prop. / Power Total	58.2	kg
Payload Mass	41.8	kg

$M_{\text{Propulsion \& Power}} \sim 58\%$

1500 m/s ΔV

Thermal Collection

- Primary concentrator
- Support structure
- Fiber optics

Thermal Storage

- PCM
- Insulation

Power

- TPV cells
- Radiator Panels

Propellant

- Liquid Ammonia

Tankage / Thruster

- Titanium Tank
- Piping
- Nozzle and Heat Exchanger
- Reinforcements



Bi-Modal System Performance Parameters
100 kg Microsatellite - 100 W continuous power draw

Silicon System		
Thermal Collection	5.3	kg
Thermal Storage	3.3	kg
Power	6.7	kg
Propellant	36.7	kg
Tankage / Thruster	6.1	kg
Prop. / Power Total	58.2	kg
Payload Mass	41.8	kg

$M_{\text{Propulsion \& Power}} \sim 58\%$

1500 m/s ΔV

Boron System		
Thermal Collection	5.4	kg
Thermal Storage	1.9	kg
Power	6.7	kg
Propellant	38.0	kg
Tankage / Thruster	6.3	kg
Prop. / Power Total	58.2	kg
Payload Mass	41.8	kg

$M_{\text{Propulsion \& Power}} \sim 58\%$

1850 m/s ΔV

Thermal Collection

- Primary concentrator
- Support structure
- Fiber optics

Thermal Storage

- PCM
- Insulation

Power

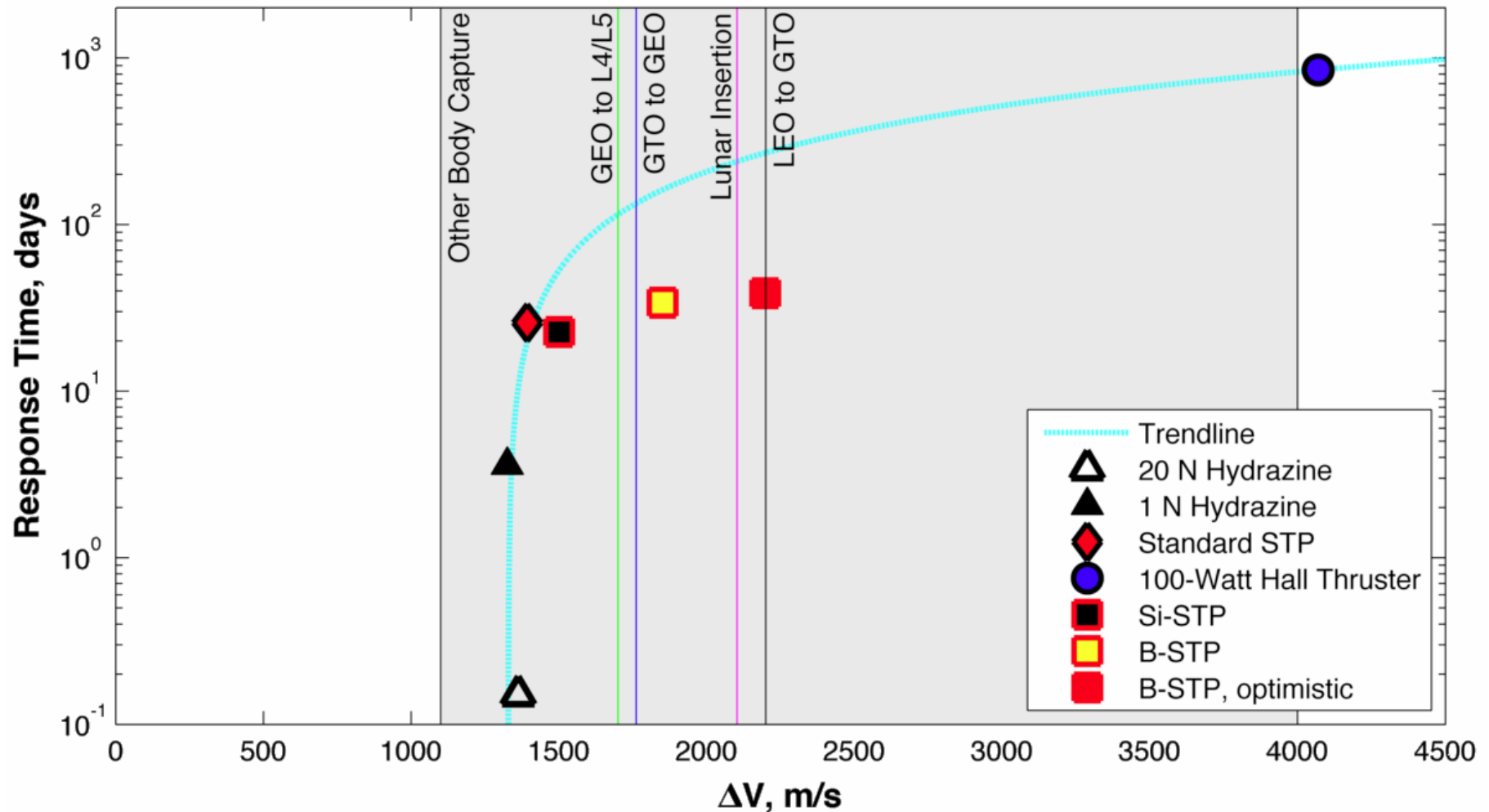
- TPV cells
- Radiator Panels

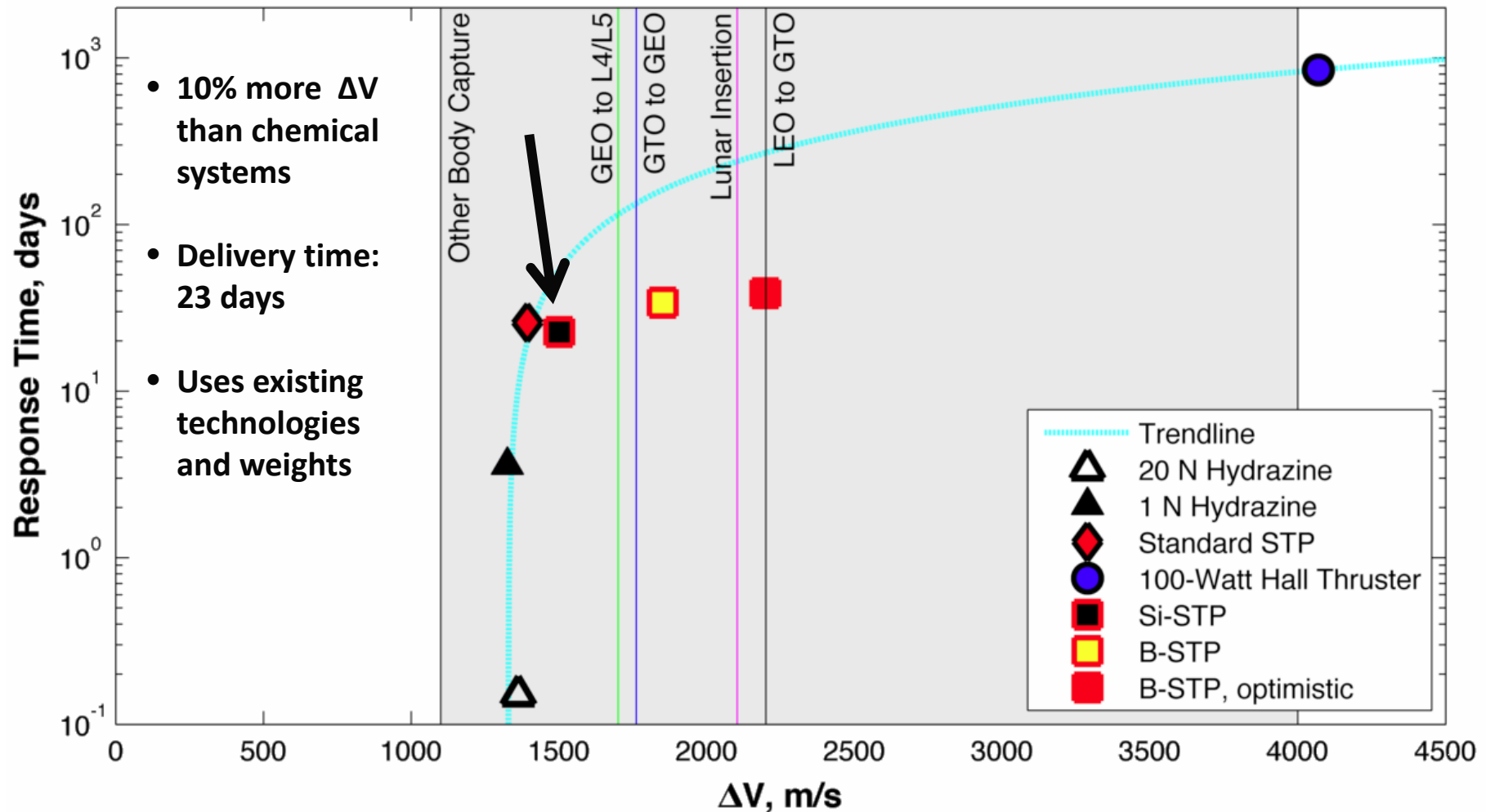
Propellant

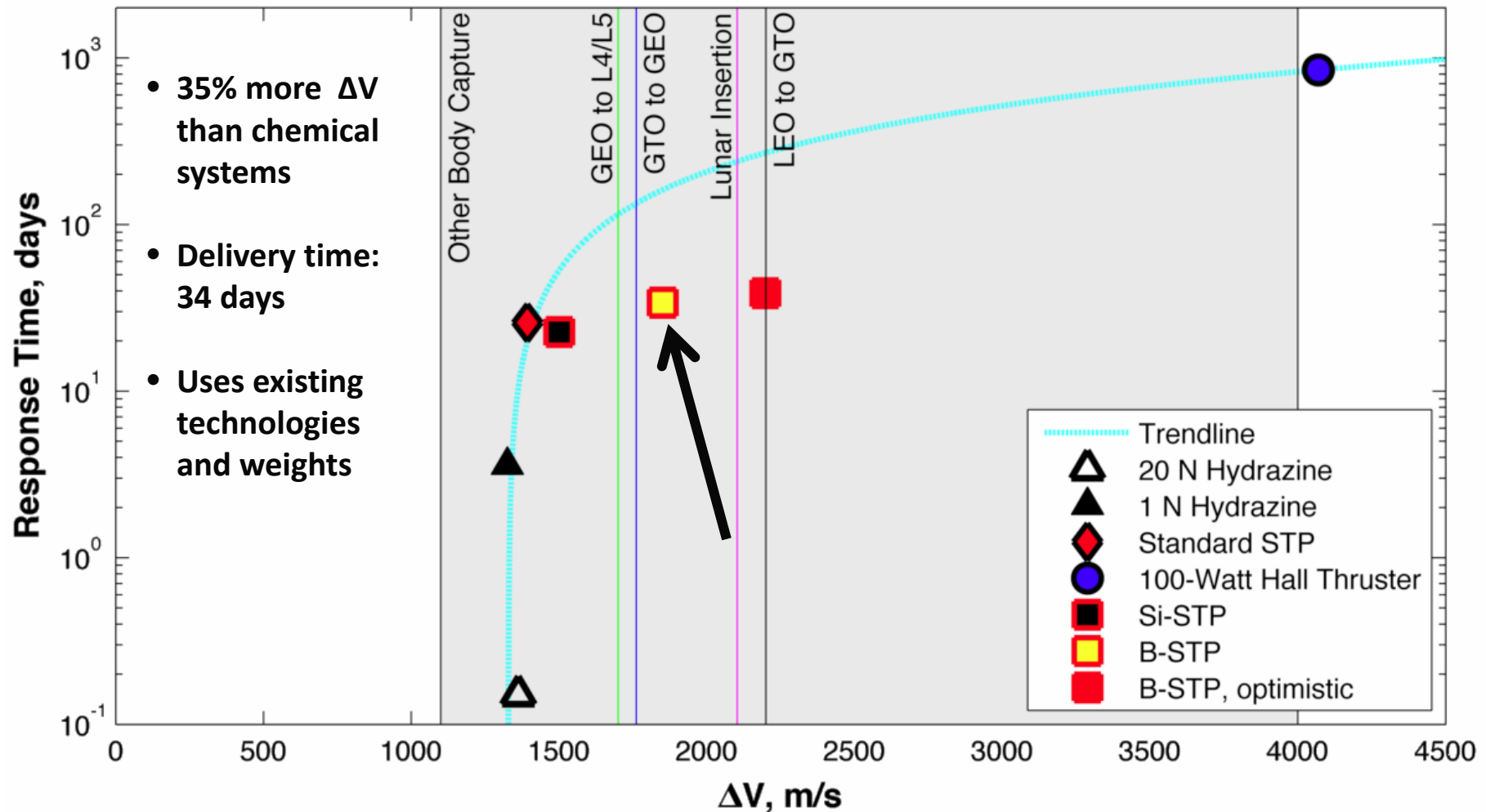
- Liquid Ammonia

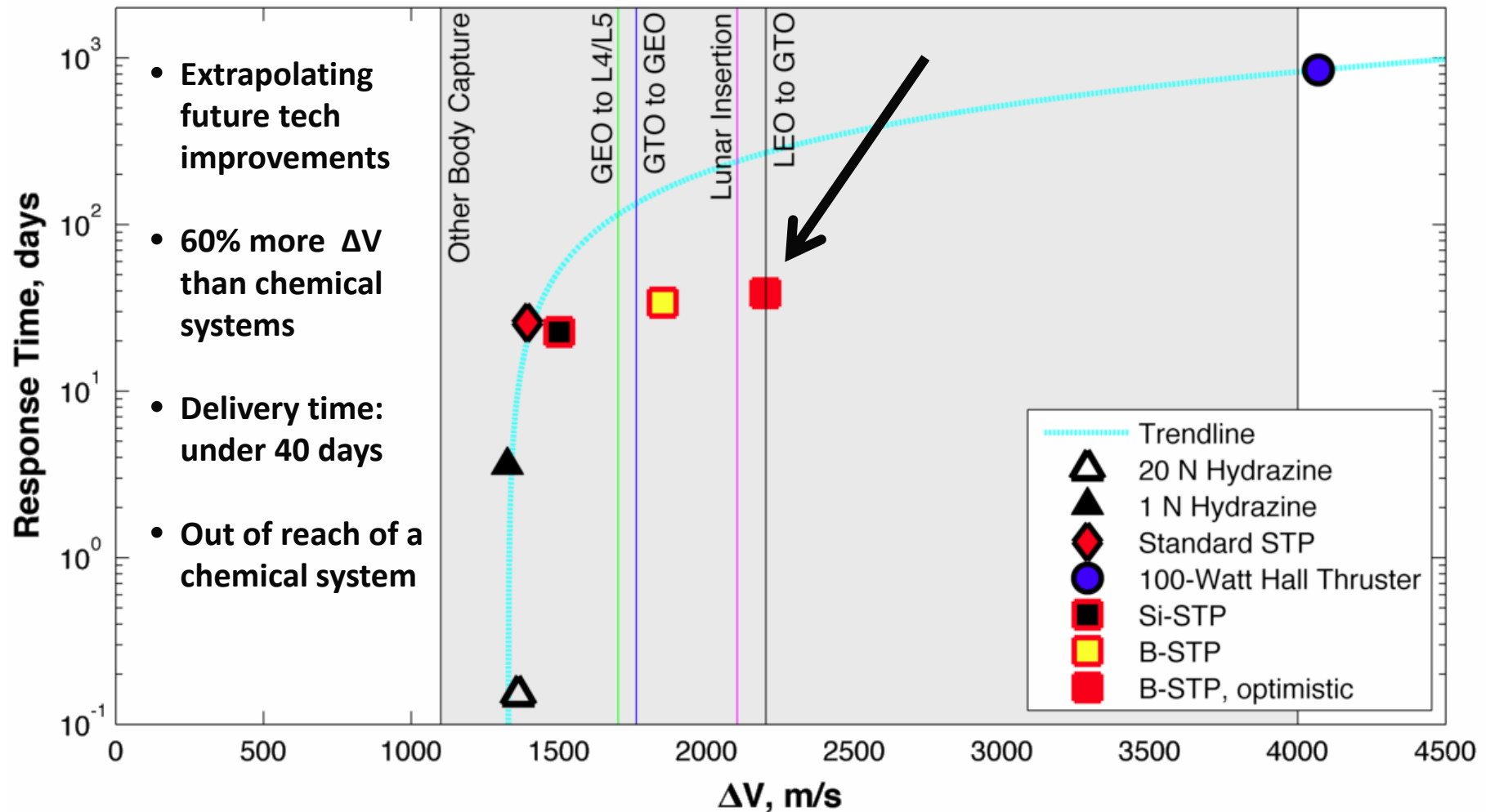
Tankage / Thruster

- Titanium Tank
- Piping
- Nozzle and Heat Exchanger
- Reinforcements









Silicon

- **Mentioned as a potential buffer / storage material for TPVs**
 - Woodall 1982 - IBM patent
 - Chubb et al. 1996 - white paper, “ideal storage material”
- **Brief mentions in the solar thermal literature**
 - Laug et al. 1995 – Initial bi-modal study
 - Kennedy 2002 – TRL level not sufficient
 - Abbot 2001 – Trade study
- **No experiments directly targeting energy storage applications**

Boron

- **Little knowledge of the material itself, let alone its use as an energy storage medium**
- **Existing experimental data is based on determining basic material properties**
 - 1960s-1970s – sealed container furnace experiments
 - 2000s – laser heated levitating drop experiments
- **Brief mentions in the solar thermal literature**
 - Shoji 1992 only considers weight savings from concentrator size reduction, says boron causes a net mass *increase*

Experimentally Demonstrate a Proof of Concept Latent Heat Thermal Energy System Using Molten Silicon

1) Facility Development

- Design and build a solar furnace at USC capable of producing molten silicon samples
- Characterize the solar furnace for accurate flux maps and power output
- Ensures experimental correlation with future spacecraft system

2) Materials Selection

- Identify suitable container materials to resist attack from molten silicon and molten boron
- Container material must demonstrate long term stability

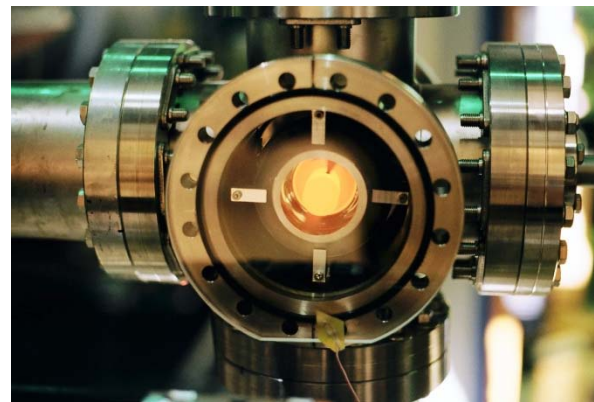
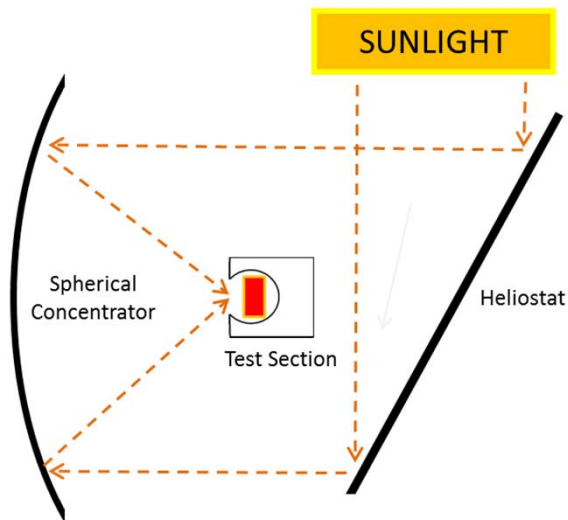
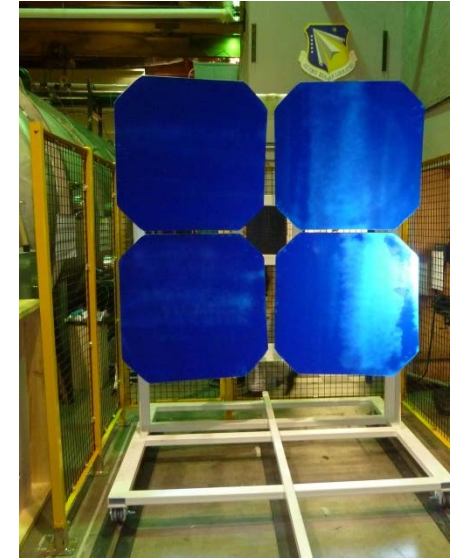
3) Modeling Capability and Analysis

- Develop sufficient modeling capability to predict experimental performance
- Asses the degrees of model fidelity required to capture essential system behaviors

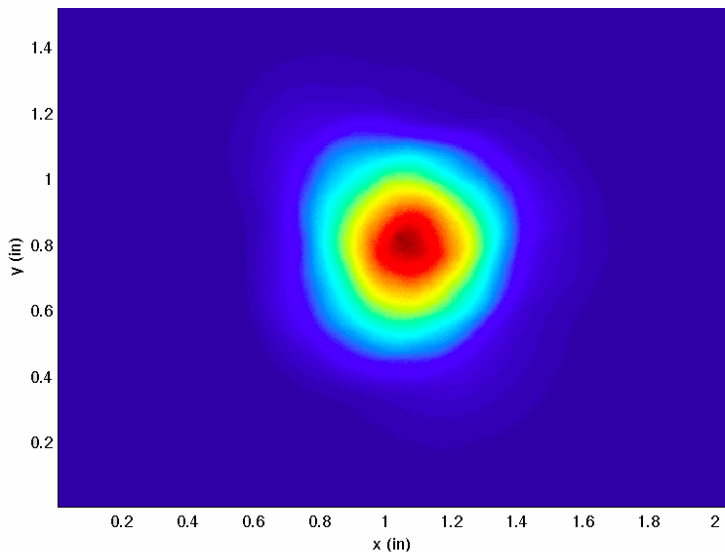
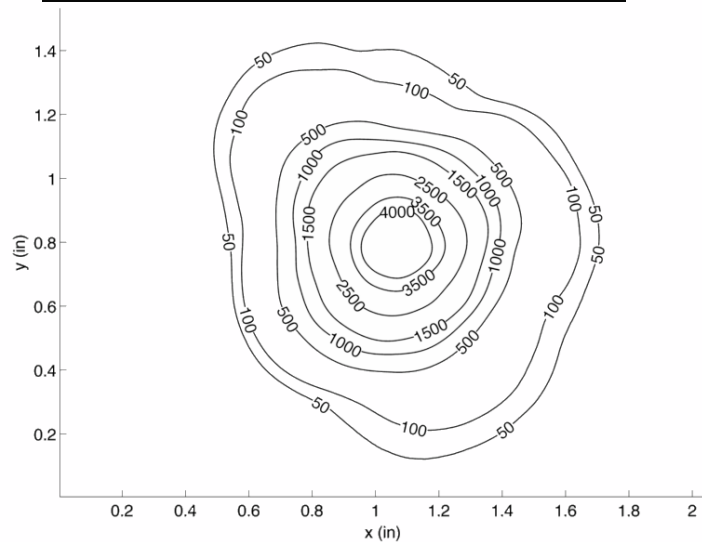
4) Experimental Demonstration

- Experimental demonstration will identify practical concerns with molten silicon and boron
- Provide experimental data for concurrent multi-physics modeling work
- Goal is to emulate a single heat exchanger channel from the ISUS experiment and demonstrate convective coupling to a latent heat medium

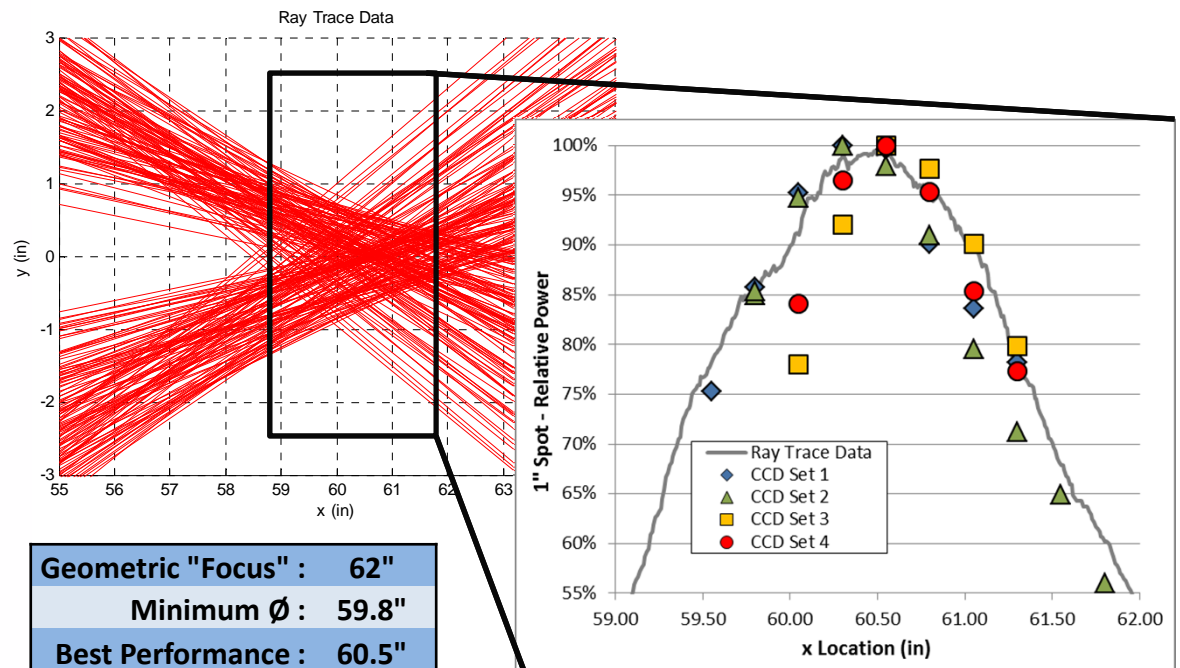
- First-surface spherical concentrator
 - $r_c = 124''$
 - SiO_2 coating optimized to the solar spectrum
 - Manufactured by DOTI Optics
- 3600 in² usable concentrator area
- 12 ft x 8 ft computer controlled heliostat
- COTS and surplus components
- Delivers 800-1100 W in a 1" spot



Solar Flux At Best Location

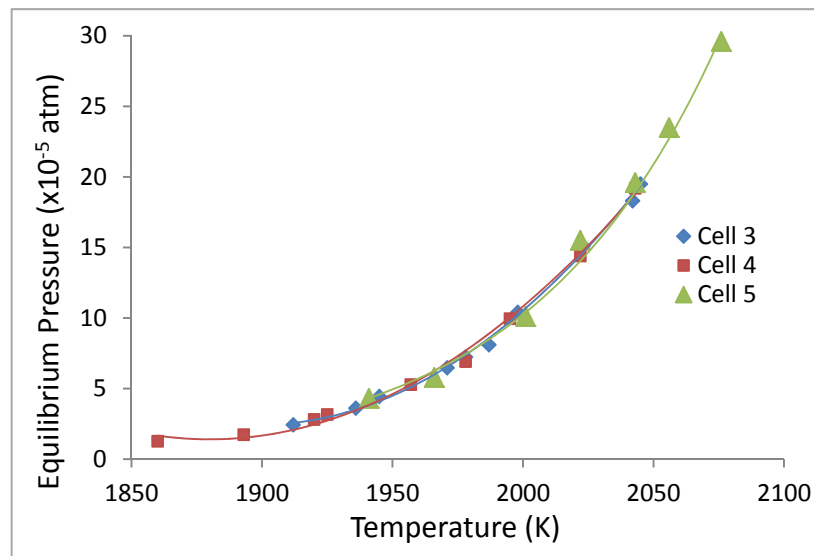


- Peak concentration ratios 4000:1
- Tailored for maximum power delivery in a 1" diameter spot
- Optimized experimental placement using CCD solar flux mapping to compensate for spherical aberrations



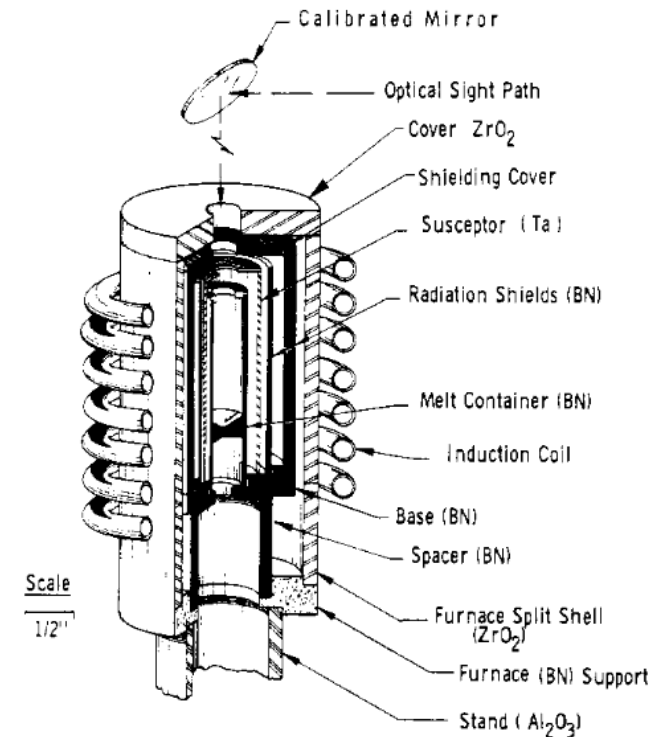
Boron

- Experimental data available for graphite, refractory metals, and boron nitride
- Boron nitride** is suggested by the literature as the most promising container material
- Concerns about dissociation at high temperature. Approx. 7 Torr at 2350 K

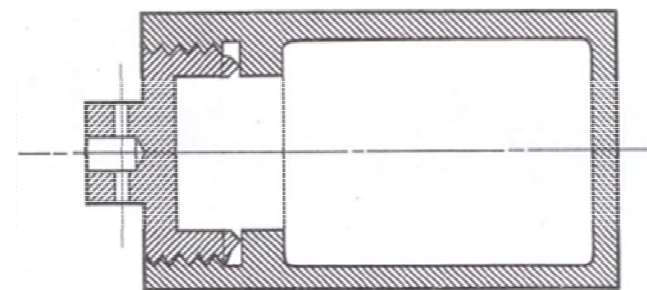


Hildenbrand 1962

DISTRIBUTION STATEMENT A: Approved for public release; distribution is unlimited. PA#XXXXX



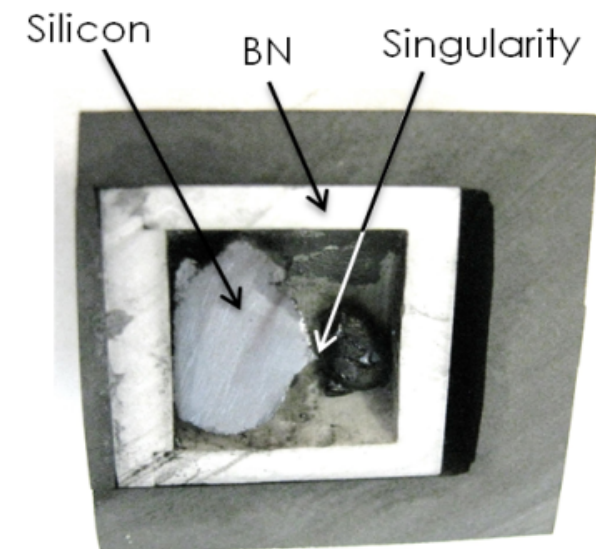
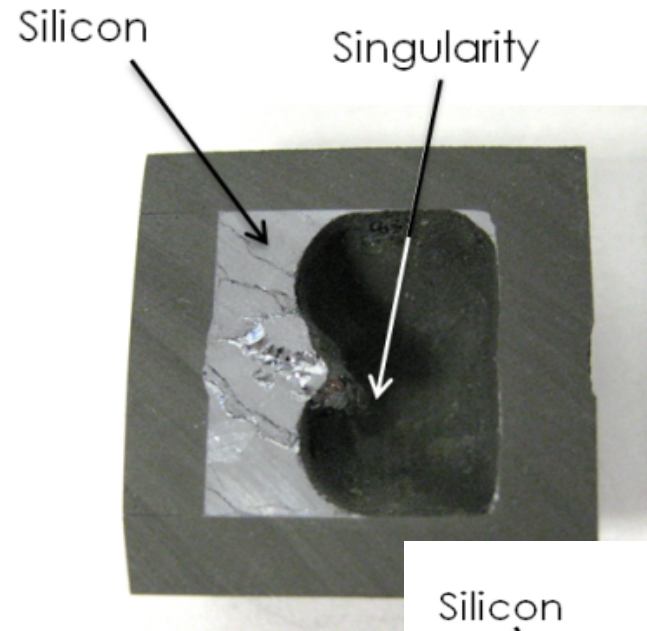
Kimpel & Moss 1968



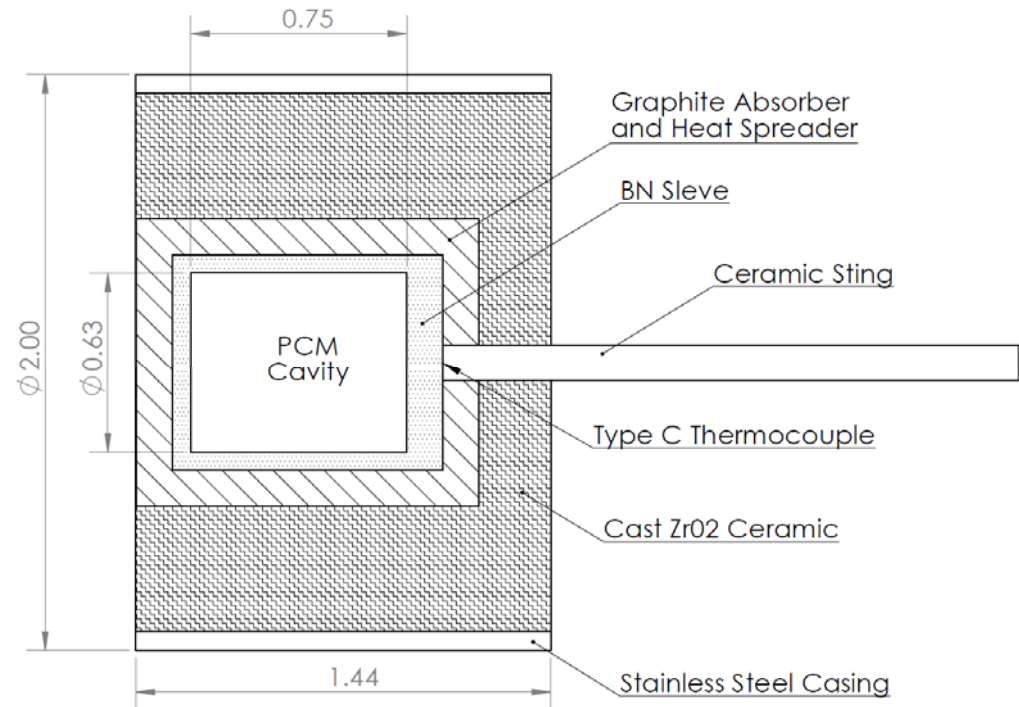
Stout et al. 1972

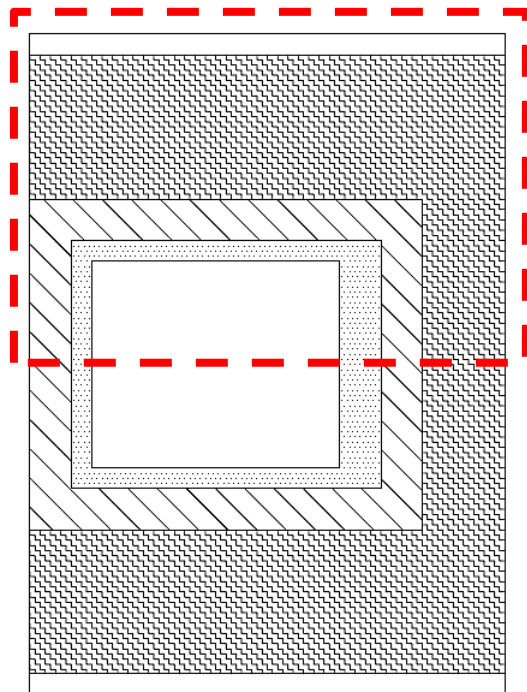
Silicon

- Possible to draw from semi-conductor industry knowledge
- **Boron nitride** has a self limiting reaction with molten silicon
 - Formation of Si_3N_4 limited at 2% boron saturation in the silicon bulk
 - Low level boron contamination expected to have little effect on silicon recrystallization
- Graphite can be used with carbon contamination on the order of 20 ppm
 - Density must be $> 1.75 \text{ g/cc}$
 - Grain size must be $< 50 \mu\text{m}$
- Approx. 10 % volumetric expansion during freezing process....



- Cylindrical geometry for ease of manufacture and simplified modeling
- Can be manufactured in house from COTS components
- Sized for 9 g of silicon, however, this is not limited by solar furnace power
- Does not make use of radiation shielding
- Integrated Type C and Type K thermocouples





t = 10 sec

t = 40 sec

t = 20 sec

t = 50 sec

t = 30 sec

t = 60 sec

1900

1800

1700

1600

1500

1400

1300

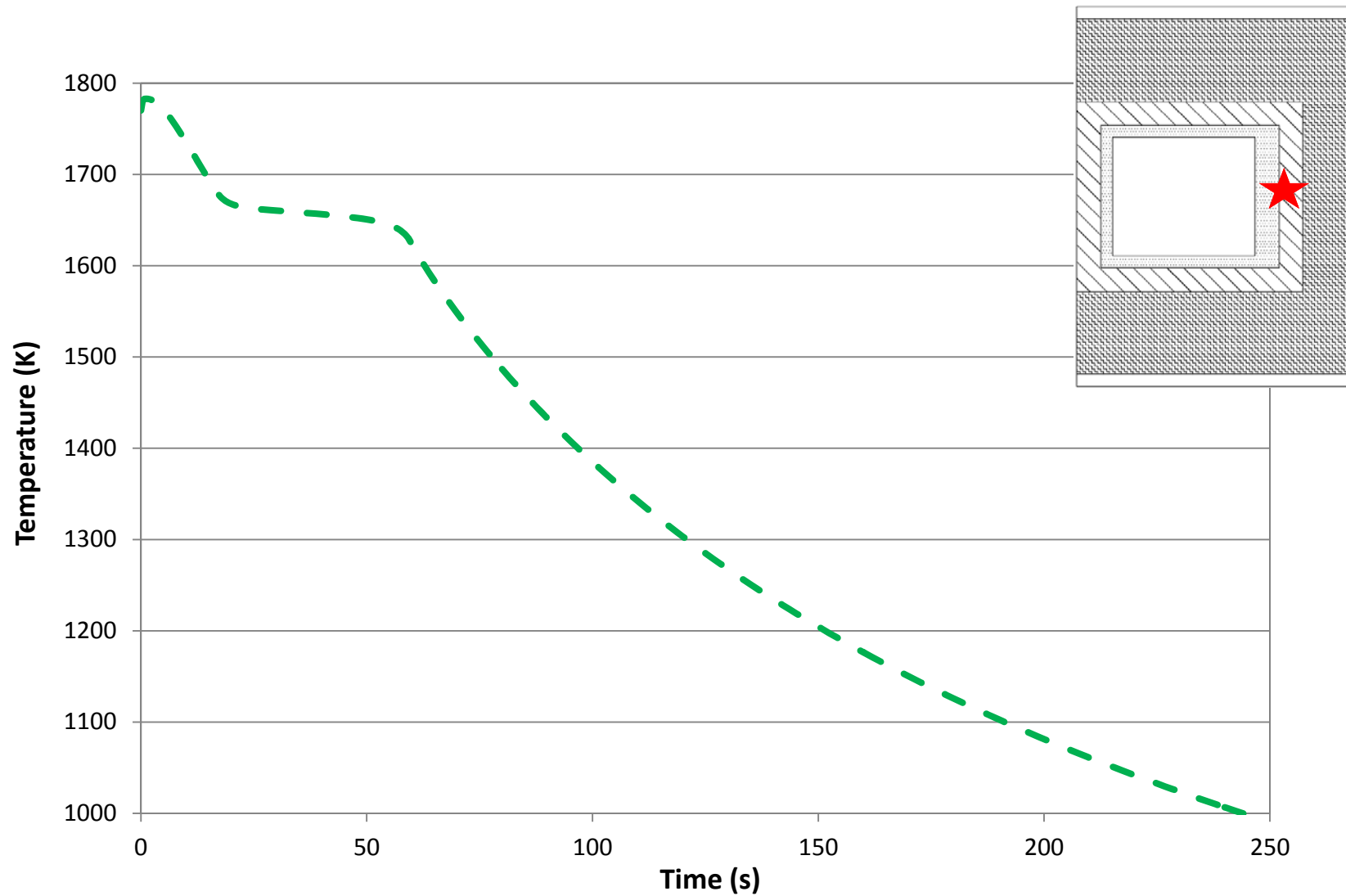
1200

1100

1000

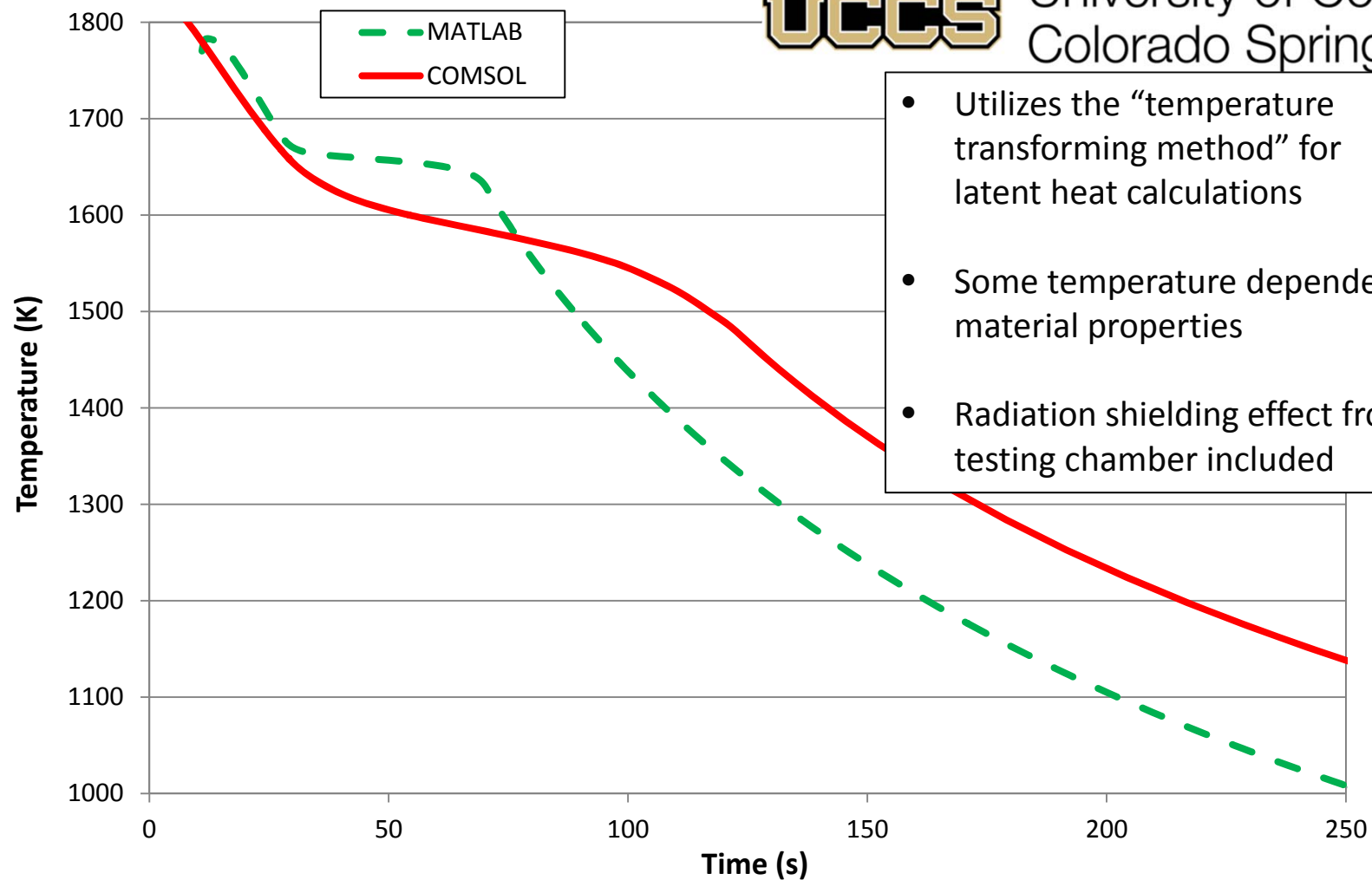
Temperature (K)

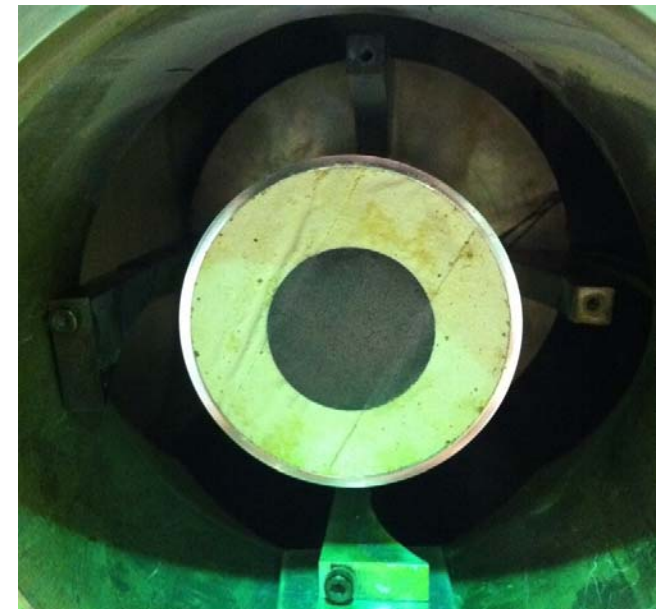
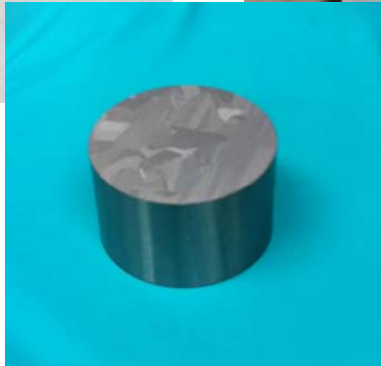
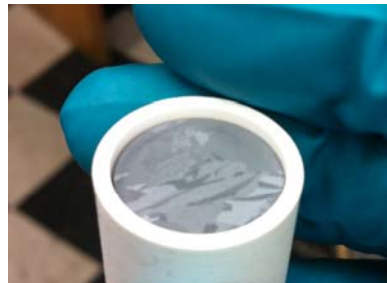
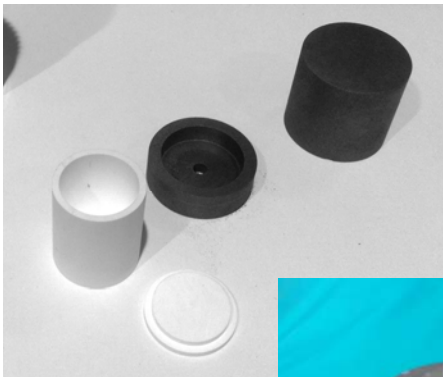
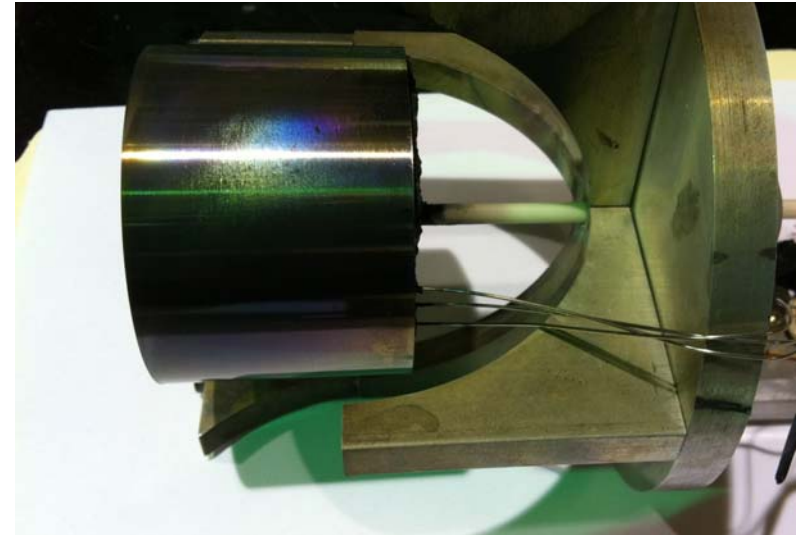
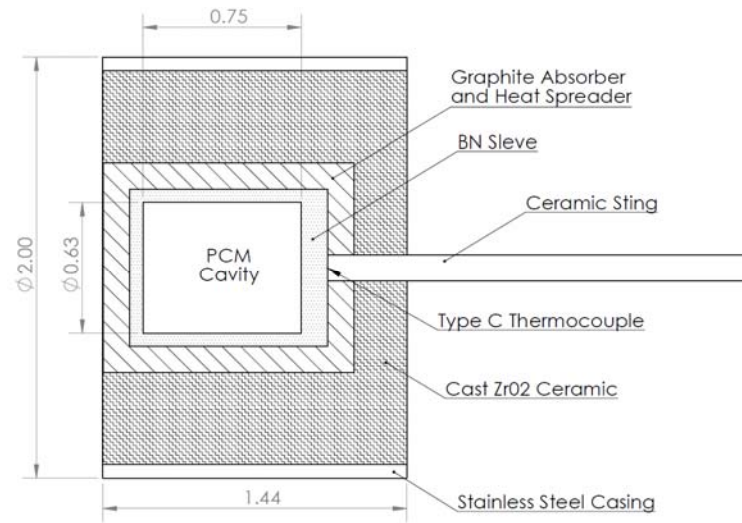
- 2D Axisymmetric about θ
- Radiation and convection boundary conditions
- Neglects PCM density change and void formation
- Latent heat handled by the “enthalpy method”



UCCS

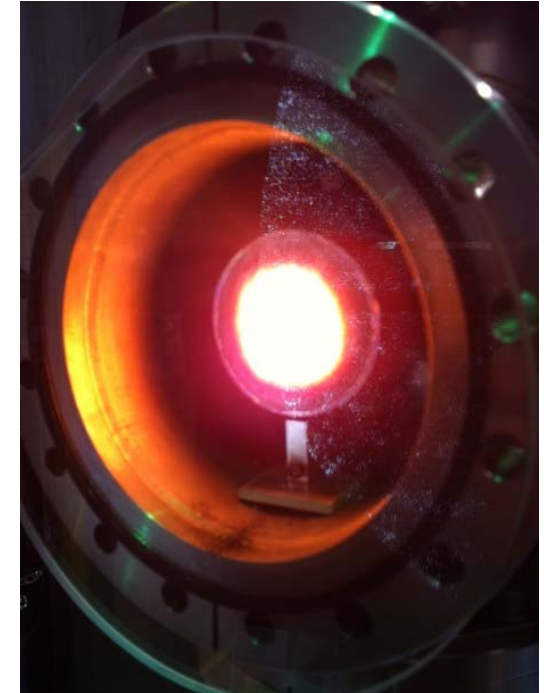
University of Colorado
Colorado Springs

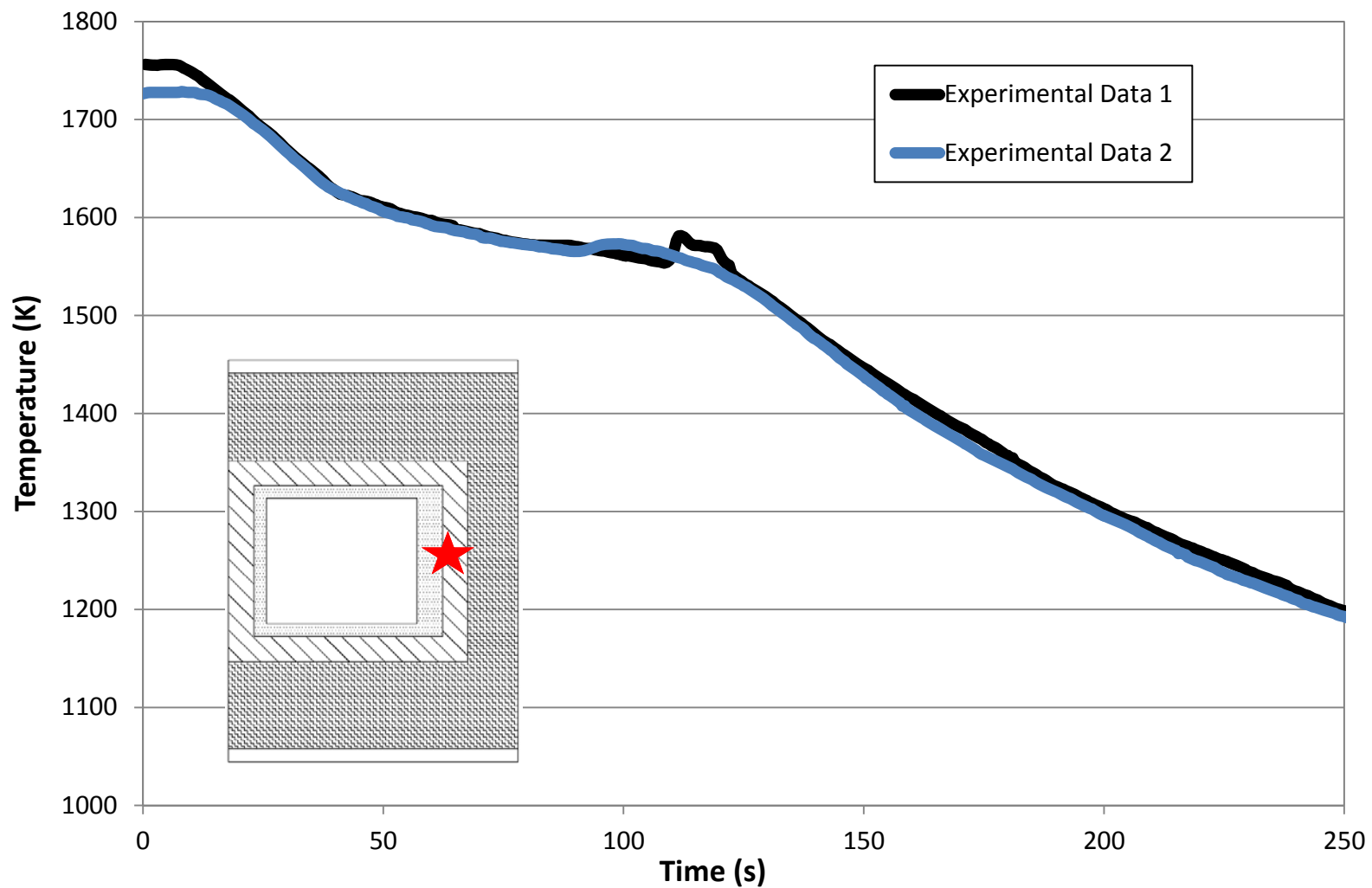


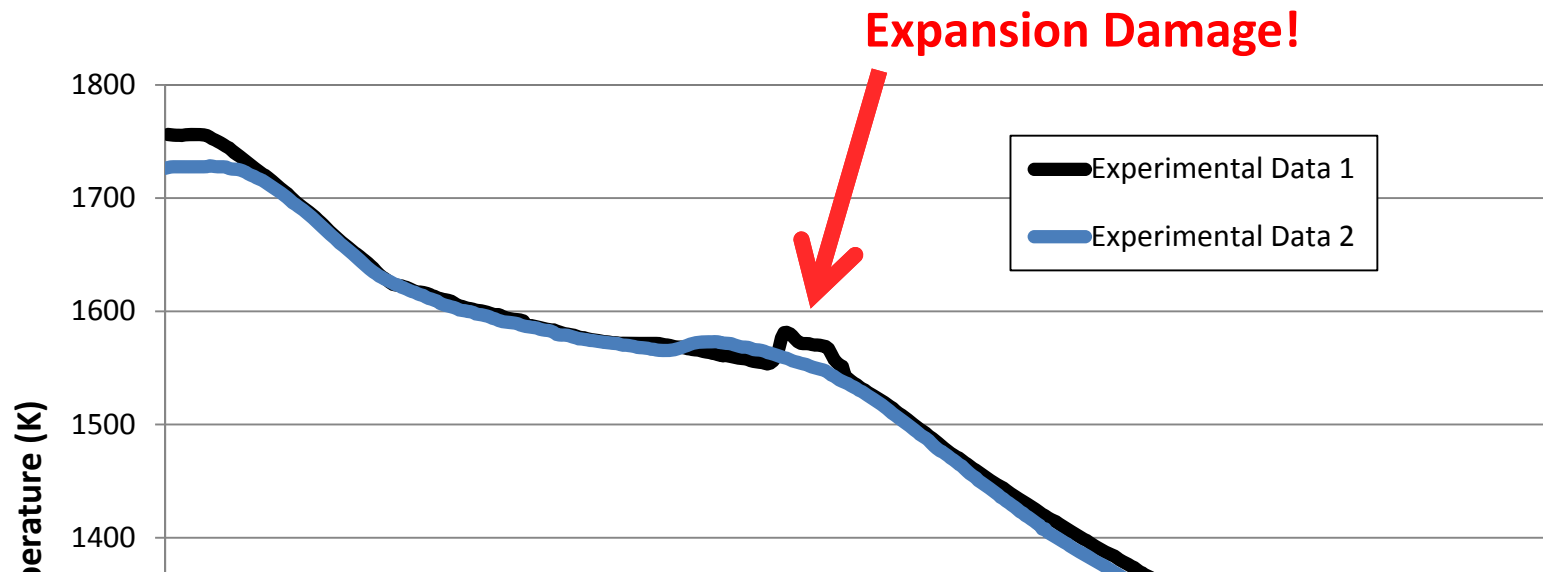


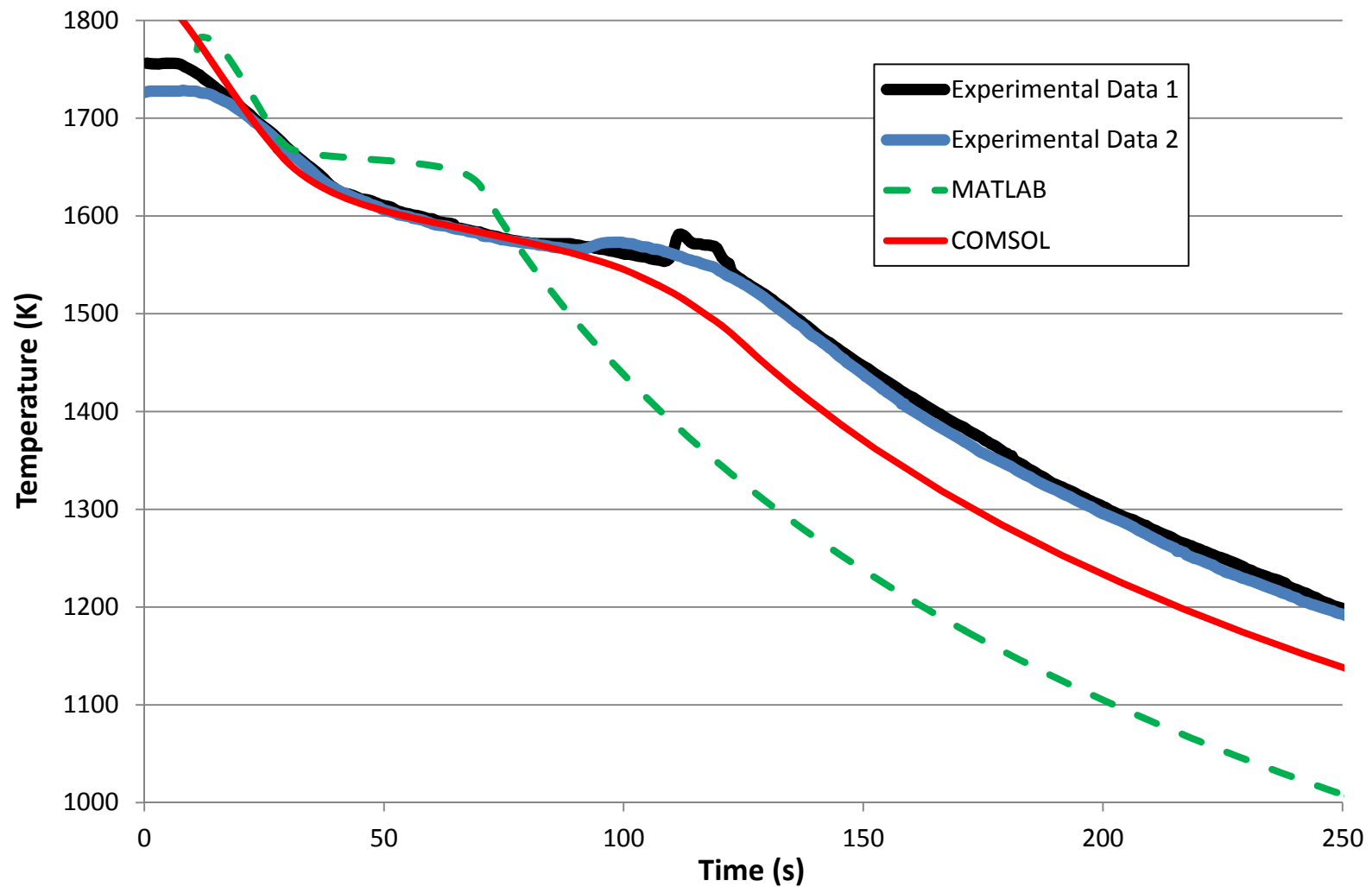
Testing Procedure

- Bake out at 300 °C using 1000 W spot lamp, at 30 mTorr to evaporate “proprietary water based binder” in the cast ZrO_2 ceramic
- Evacuate to 30 mTorr at ambient temperature, then heat “on-sun” to 300 °C to ensure no gas is trapped in the test section prior to seal tightening due to thermal expansion
- Fill chamber with 150 Torr of Argon
 - Required to suppress $\text{ZrO}_2 + \text{C}$ reaction
 - Prevents irreparable damage to quartz chamber window
- Gradually increase power until thermal equilibrium is achieved
- Use “shutter curtain” to quickly cut power and record cooling curve



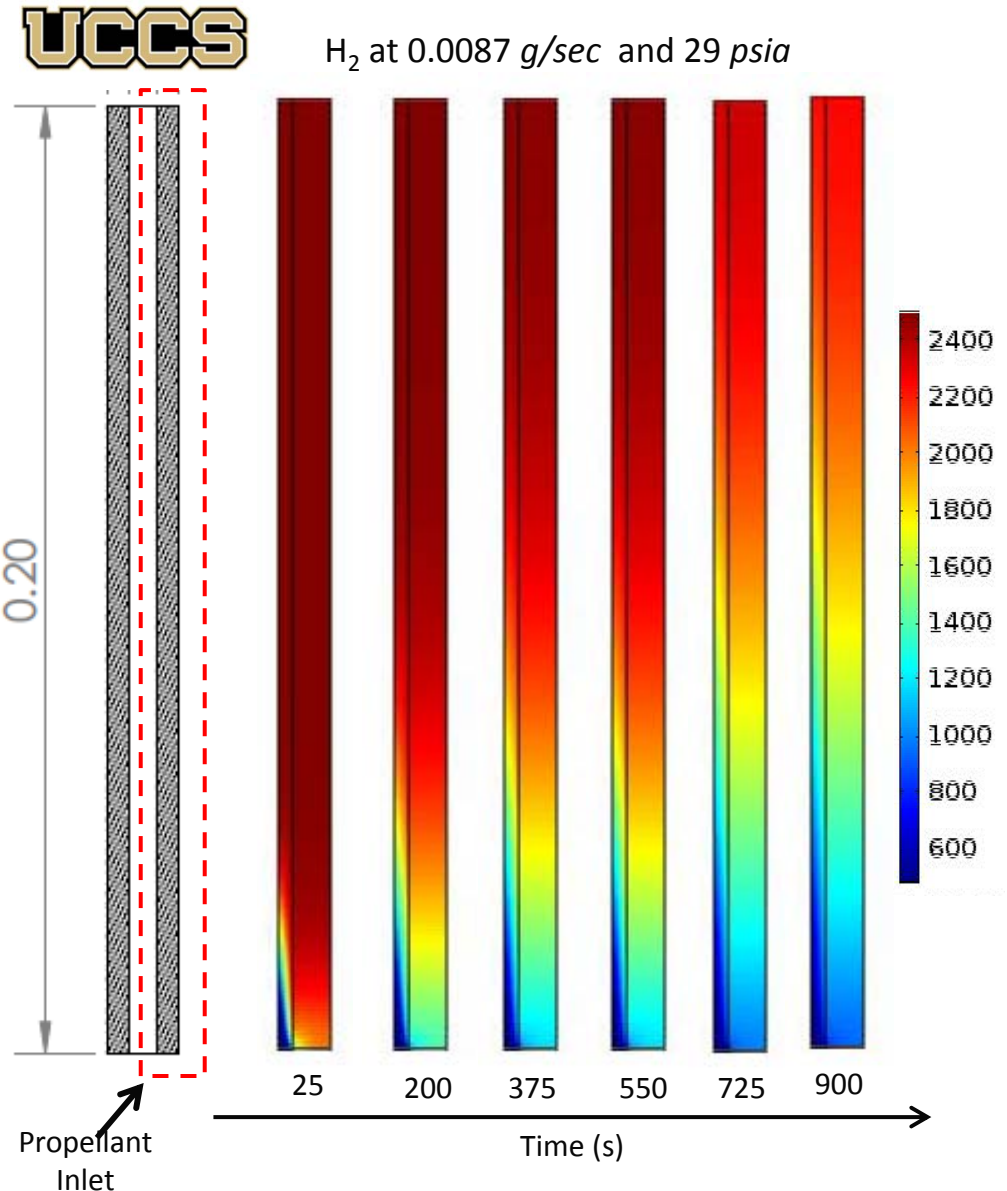






Convective Coupling

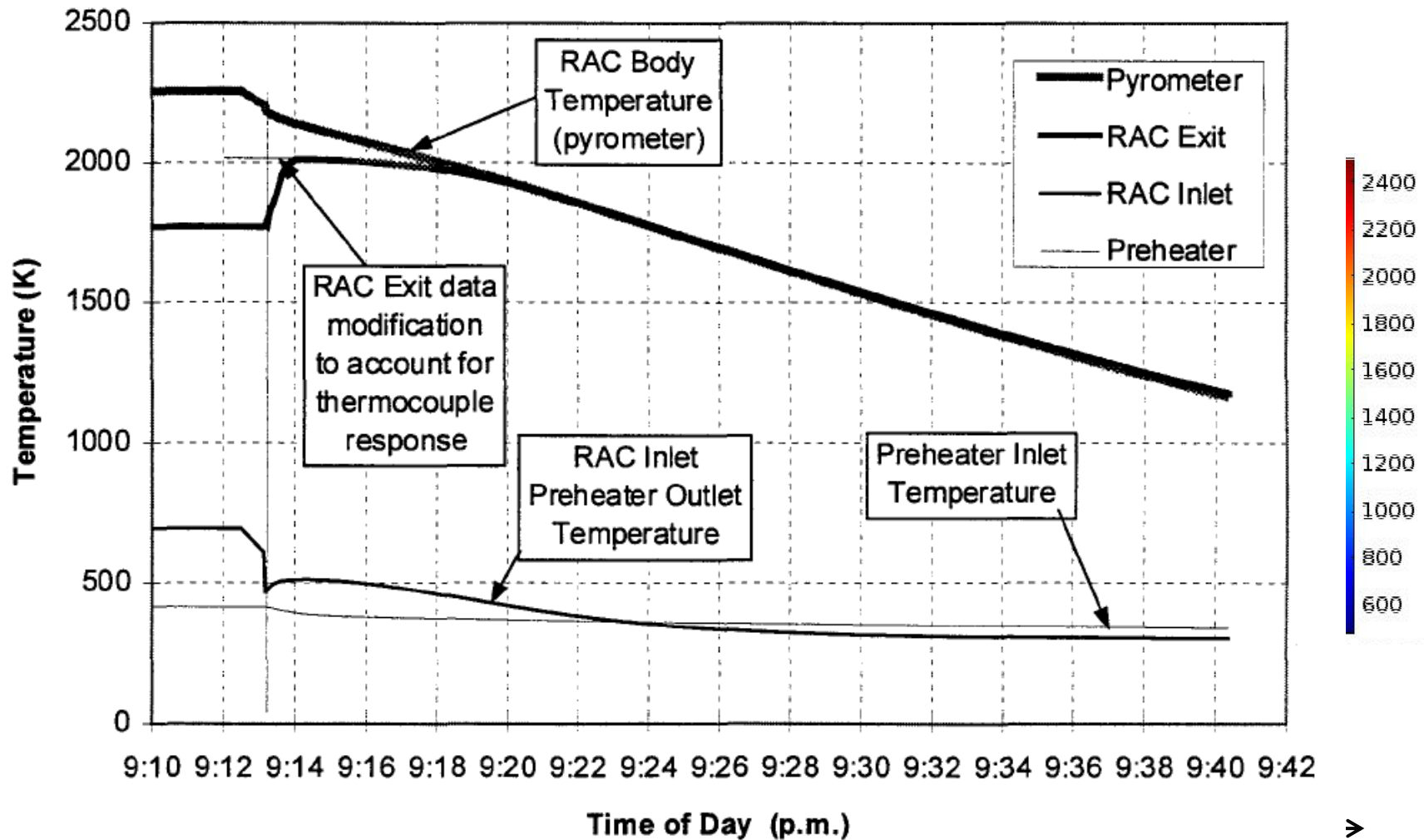
- The ISUS system was capable of maintaining a constant temperature with a sensible heat medium due to “extra length” being designed into the heat exchanger
- The design spec of the ISUS RAC has the potential for 0.72 MJ/kg with a 600 K ΔT (double the original design spec)
- In reality, achieves 0.46 MJ/kg if the steady output region is considered “usable”
- To date, no discussion of latent heat thermal energy storage discusses **advantageous convective coupling**
- Will use commercial multi-physics software (Star-CCM+) to replicate a ISUS heat exchanger channel and switch storage to latent heat
- Seek a quantification of convective coupling benefit



Convective Coupling

UCCS

H₂ at 0.0087 g/sec and 29 psia



- The cons med into

- The pote the c

- In re outp

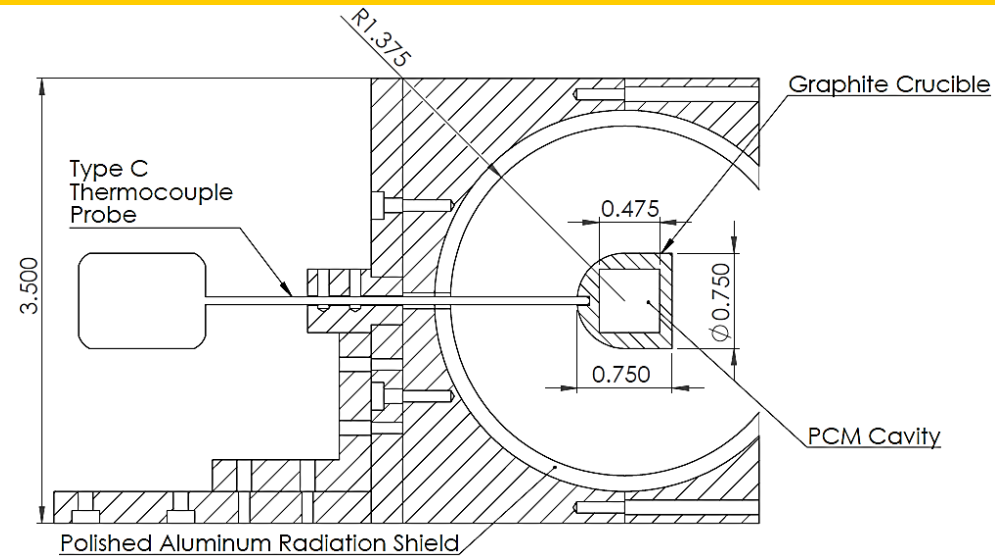
- To d ener **conv**

- Will (Star chan

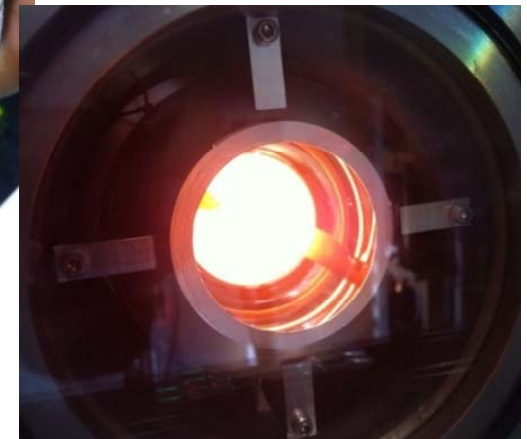
- Seek benefit

Radiation Shielding

- Radiation shielding will be required to increase molten silicon yields
- Testing was performed with spherical radiation shields during solar furnace development
- Goal was to reproduce results published by Steinfeld and Fletcher – found that assumptions of iso thermal test sections were inaccurate
- Demonstrated shielding efficiency of approx. 55% with hand polished aluminum shields
- Must be integrated into predictive models
- Ray tracing code from AFRL has been written to produce point to point view factors for spherical and cylindrical geometries



$$T_{Max} \approx \left[\dots \left(\frac{1}{1 - \eta_{Shielding}} \right)^{1/4} \right]$$

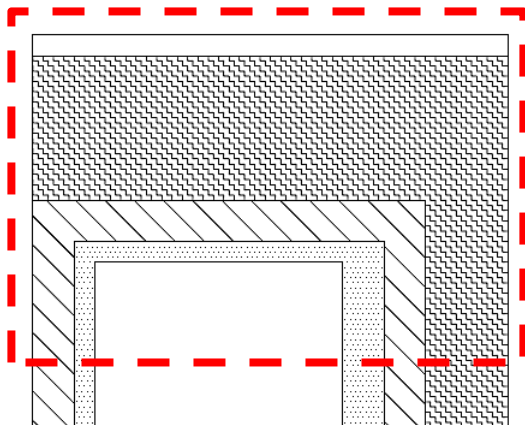
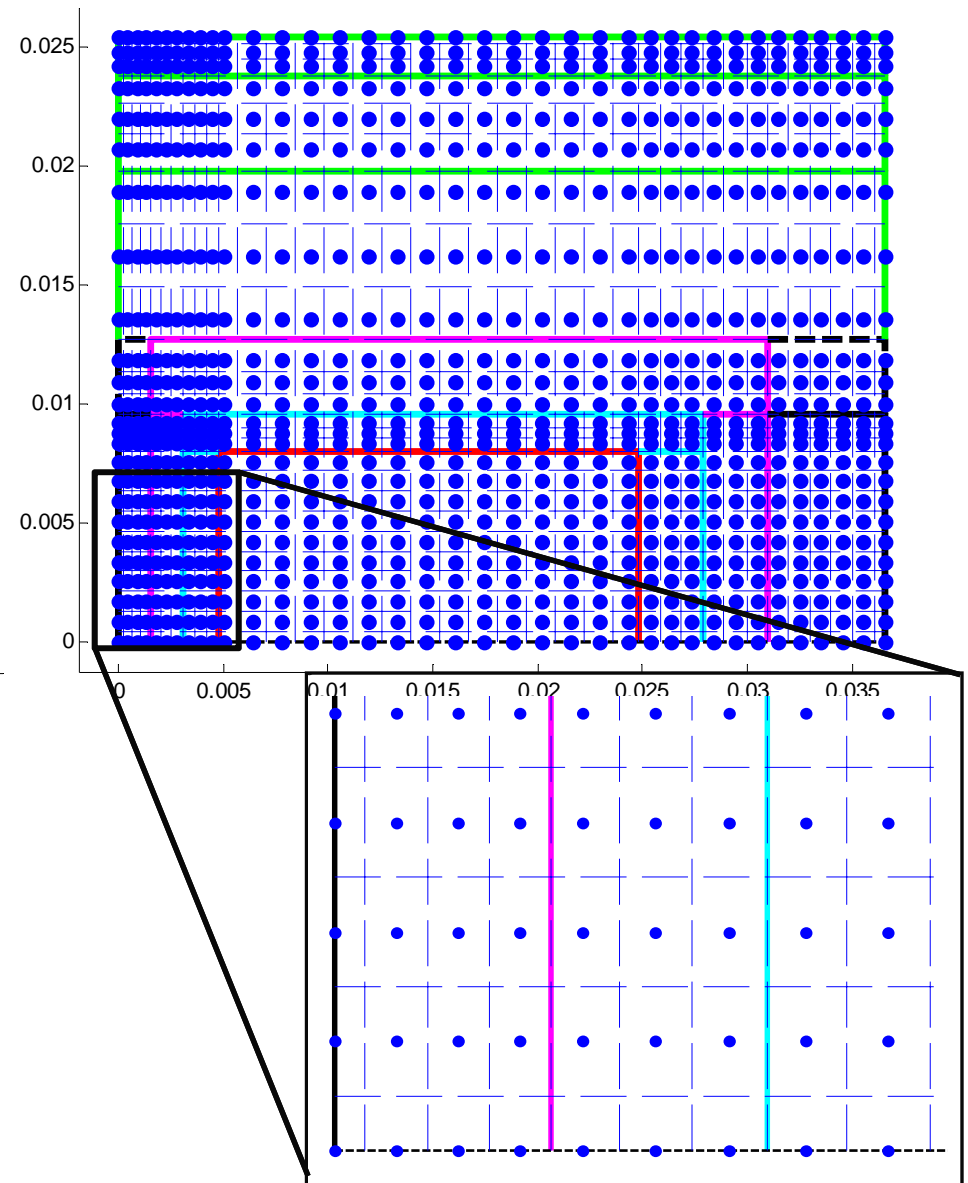
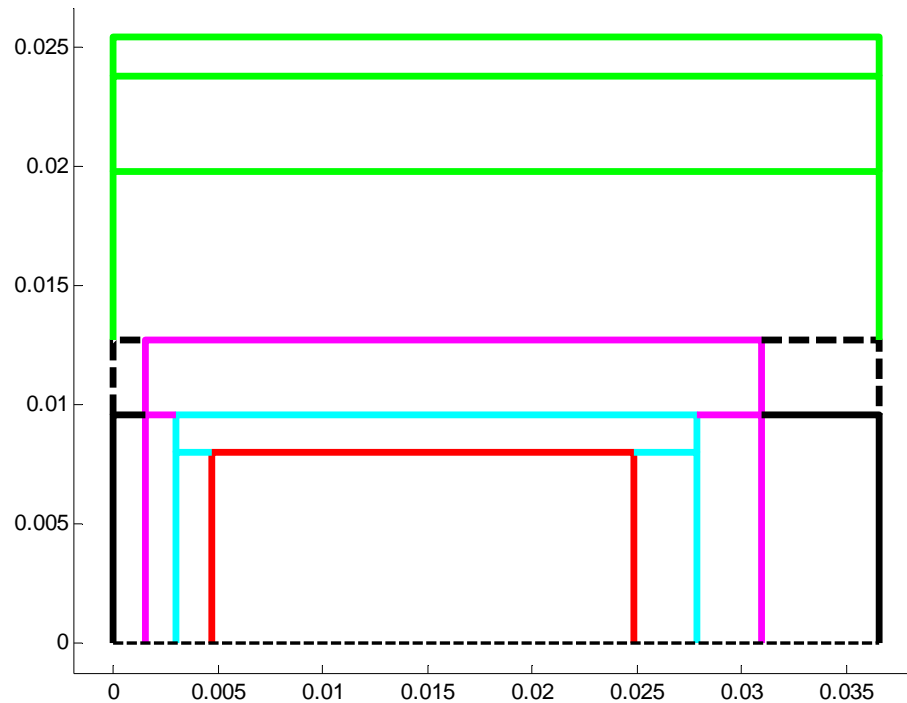




Project Conclusion

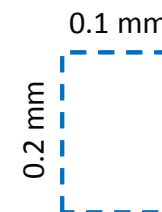
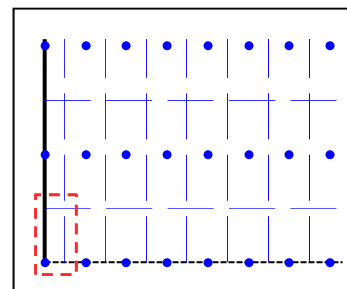
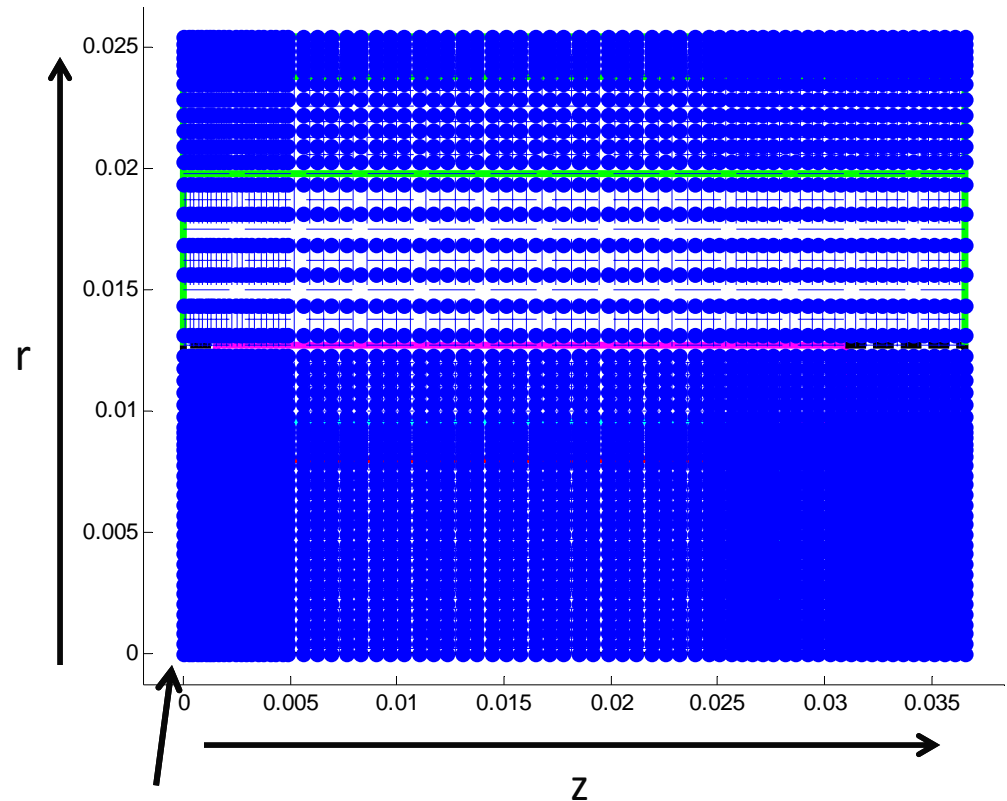
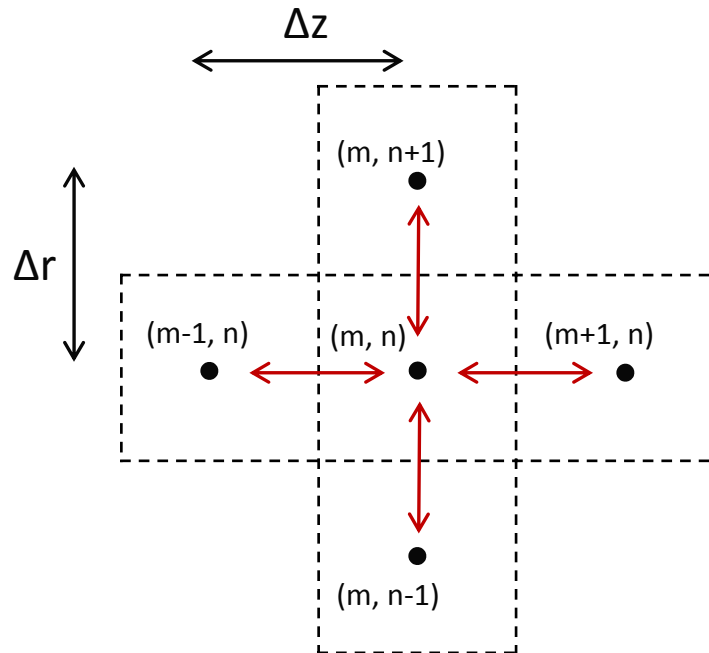
- Emulate an ISUS heat exchanger channel and experimentally demonstrate sensible and latent heat storage options
- Requires increasing furnace performance and insulation techniques
 - Replacement of heliostat mirrors will yield a 30% power increase
 - Secondary concentrator can increase c. ratio to > 10,000:1
 - Addition of radiation shielding and potentially CBCF insulation
- When complete, experiments will bring latent heat thermal energy storage for STP to a similar TRL level as sensible heat options
- This research is the most thorough investigation into high temperature latent heat thermal energy storage and will provide a road map for future solar thermal system designers





DISTRIBUTION STATEMENT A: Approved for public release; distribution is unlimited. PA#XXXXXX

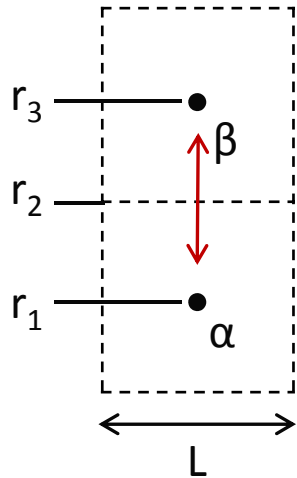
- 3700 Nodes
- $dt = 0.00025$ seconds
- Approx. 14 hours runtime for a 300 second simulation



$$V = 1.3 \times 10^{-5} \text{ cc}$$

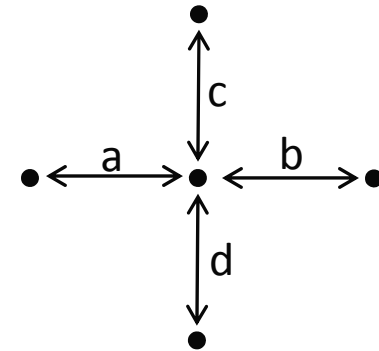
$$m = 2.65 \times 10^{-5} \text{ g}$$

Conduction in the “r” Direction



$$q = \frac{(T_\beta - T_\alpha)}{\frac{\ln(r_2/r_1)}{2\pi L k_\alpha} + \frac{\ln(r_3/r_2)}{2\pi L k_\beta}}$$

All geometric terms are offloaded into coefficient matrices to speed computations



At Each Time Step

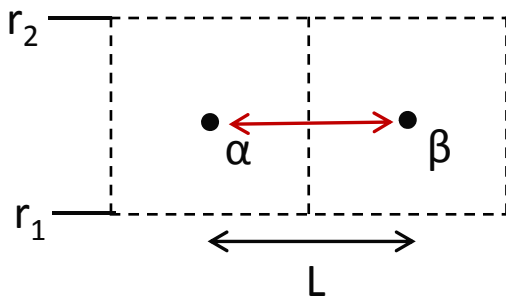
$$q_{net} = q_{left} + q_{right} + q_{down} + q_{up}$$

$$\Delta T = \frac{q_{net} dt}{mc_p}$$

Node With PCM

$$\Delta T = \frac{q_{net} dt}{mc_p} + LatentHeat(rr, zz)$$

Conduction in the “z” Direction



$$q = \frac{A(T_\beta - T_\alpha)}{L(1/k_\alpha + 1/k_\beta)}$$

$$A = \pi(r_2^2 - r_1^2)$$

Radiation Boundary Condition

$$q_{rad} = -\sigma \epsilon A (T_{node}^4 - T_{amb}^4)$$

$$q_{net} = q_{left} + q_{right} + q_{down} + q_{up} + q_{rad} + q_{conv}$$

$$\Delta T = \frac{q_{net} dt}{mc_p}$$

Convective Boundary Condition

$$q_{conv} = -hA(T_{node} - T_{amb})$$

Vertical Plate $\rightarrow h \approx 6.7 \text{ (W/m}^2\text{K)}$

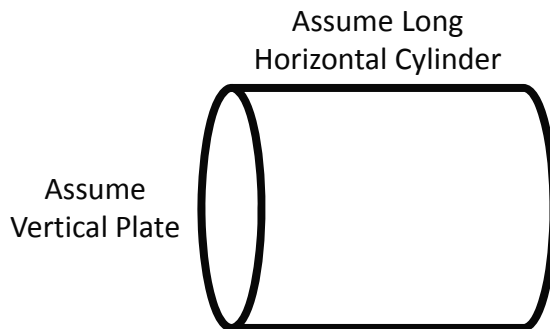
$$h = \frac{k}{L} \left(0.825 + \frac{0.387 Ra_L^{1/6}}{(1 + (0.492/Pr)^{9/16})^{8/27}} \right)^2 \quad (\text{Churchill and Chu})$$

Assume laminar flow with Argon at 500 K and 150 Torr ($Ra_L = 10^6$)

Horizontal Cylinder $\rightarrow h \approx 5.7 \text{ (W/m}^2\text{K)}$

$$h = \frac{k}{D} \left(0.6 + \frac{0.387 Ra_D^{1/6}}{(1 + (0.559/Pr)^{9/16})^{8/27}} \right)^2 \quad (\text{Churchill and Chu})$$

Assume laminar flow with Argon at 500 K and 150 Torr ($Ra_L = 10^6$)

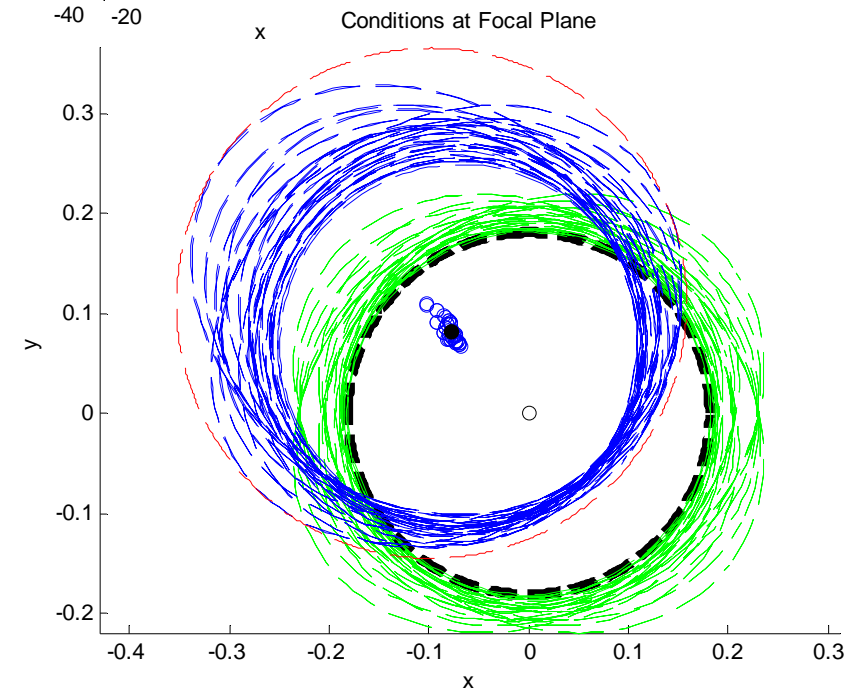
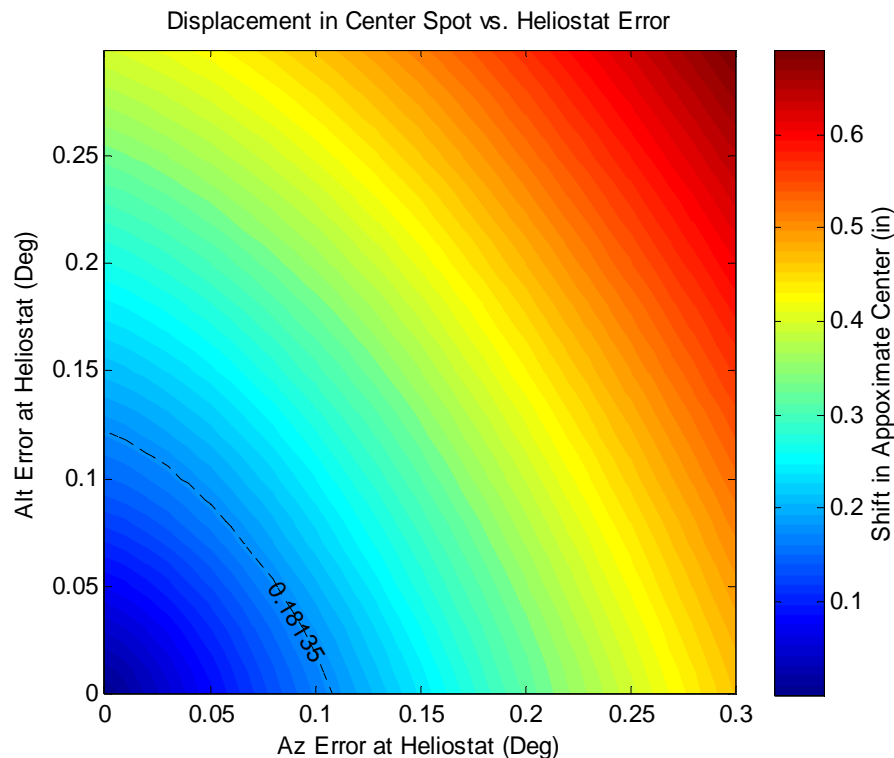
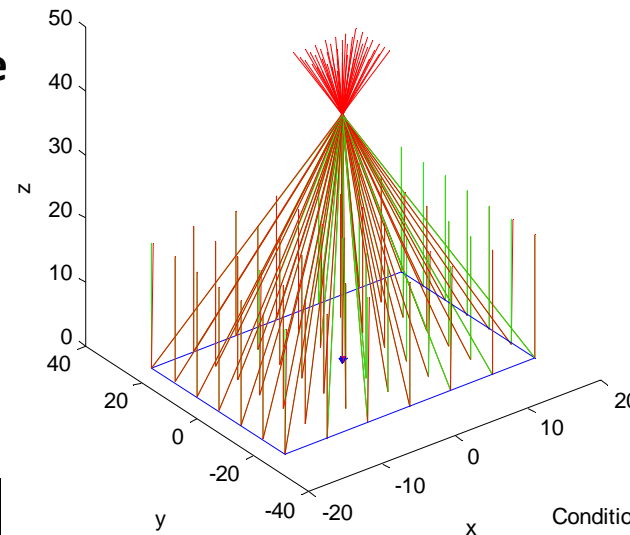


Accuracy Requirements in the Literature

- $\pm 0.3^\circ$ - *Hukuo 1957*
- $\pm 0.1^\circ$ - *Ethridge 1979*
- $\pm 0.5^\circ$ - *Holmes 1995*
- $\pm 0.1^\circ$ - *Kennedy 2004*

Note idea image
for a parabolic
concentrator

$$d = 2f \sin(\theta_{sun}/2)$$



Hukuo and Mii 1957

FIG. 1 — Section of a parabolic mirror.

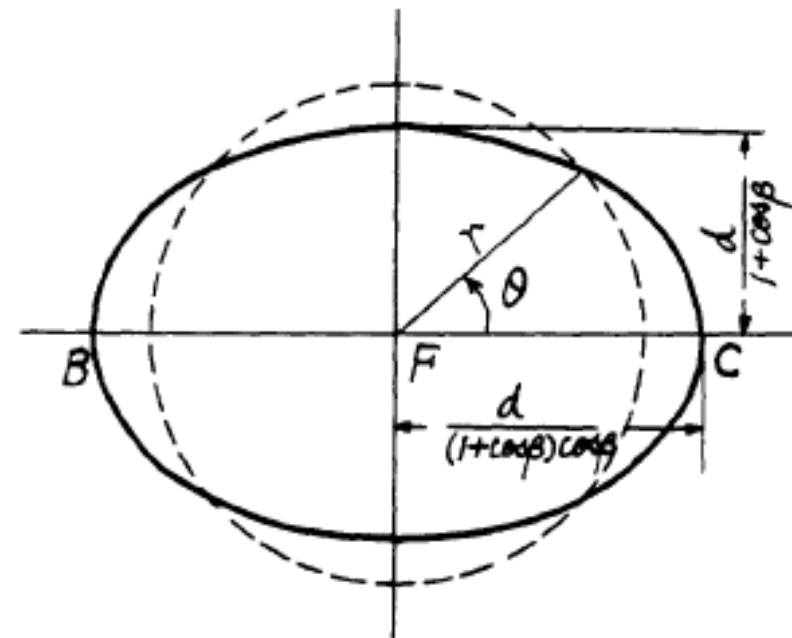
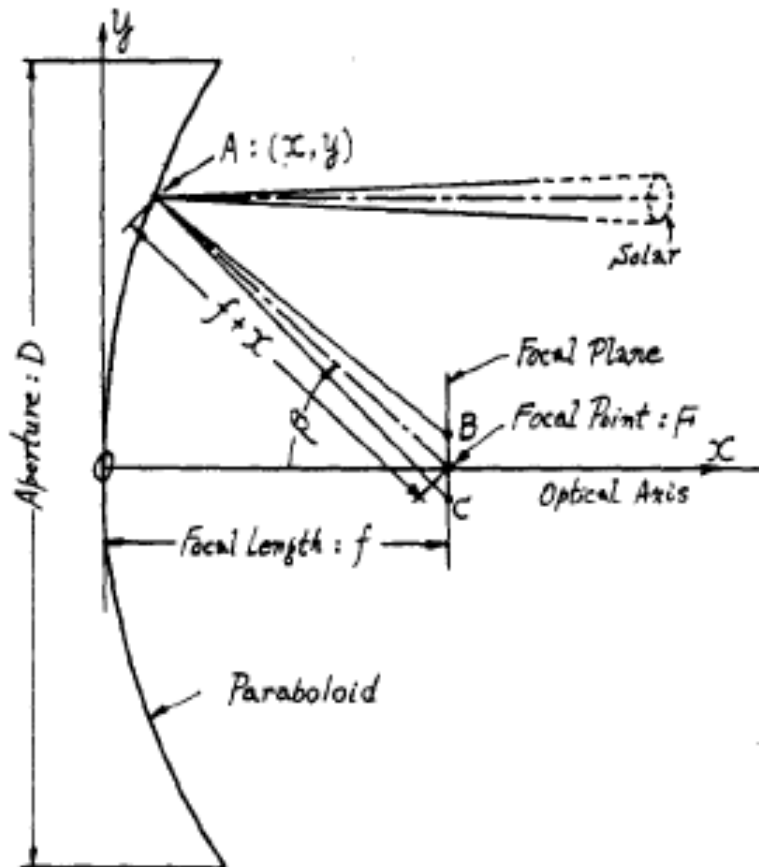
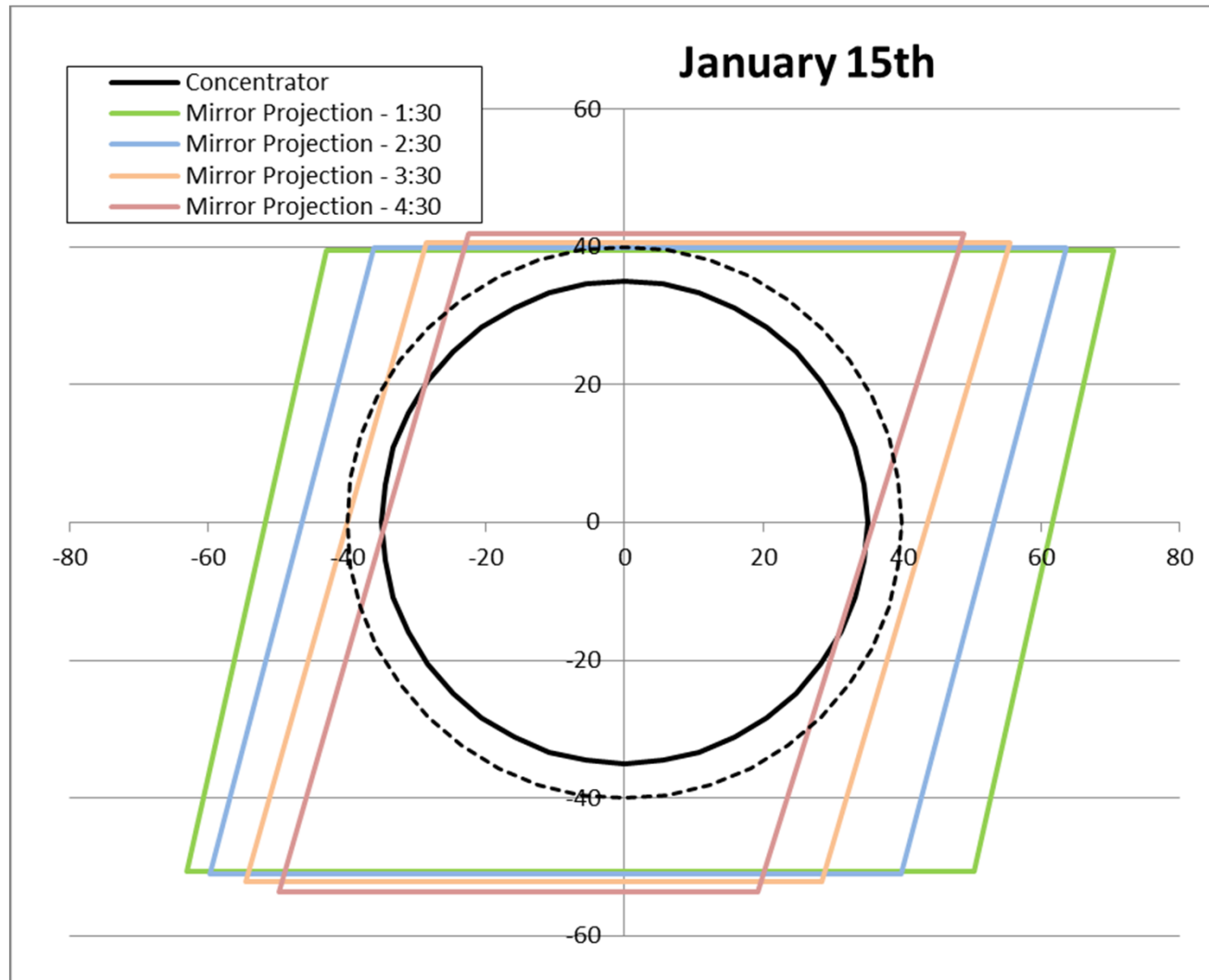
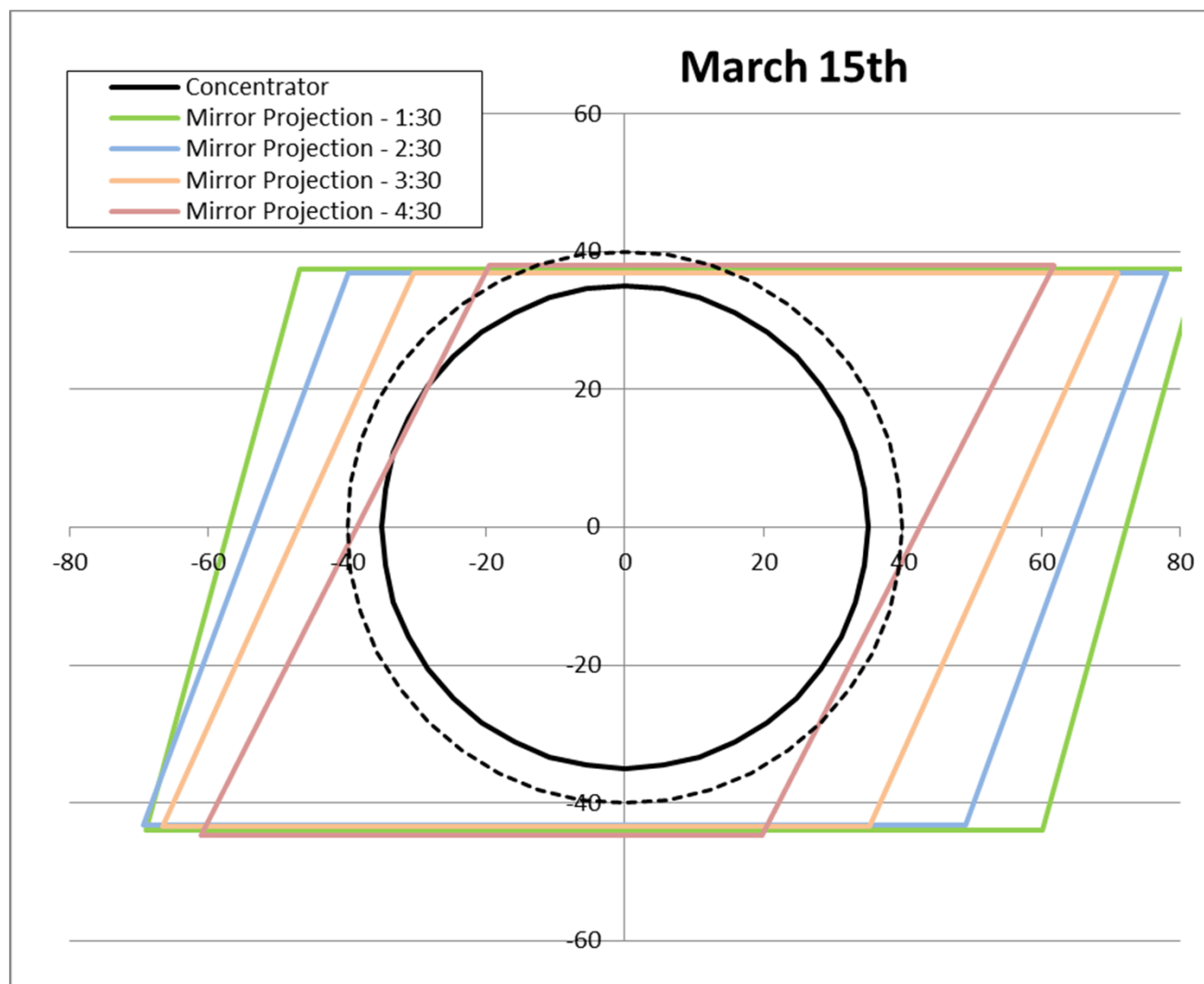
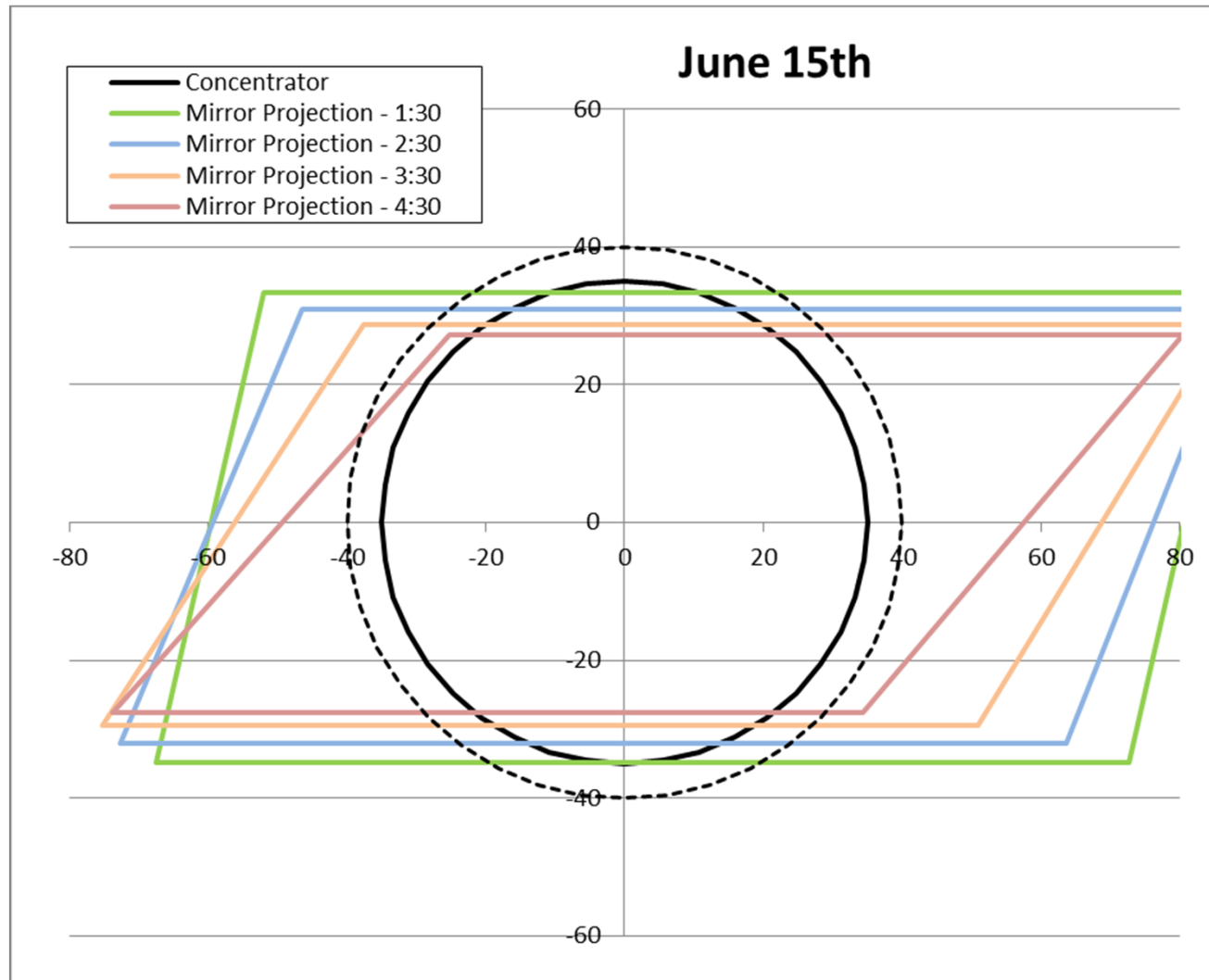


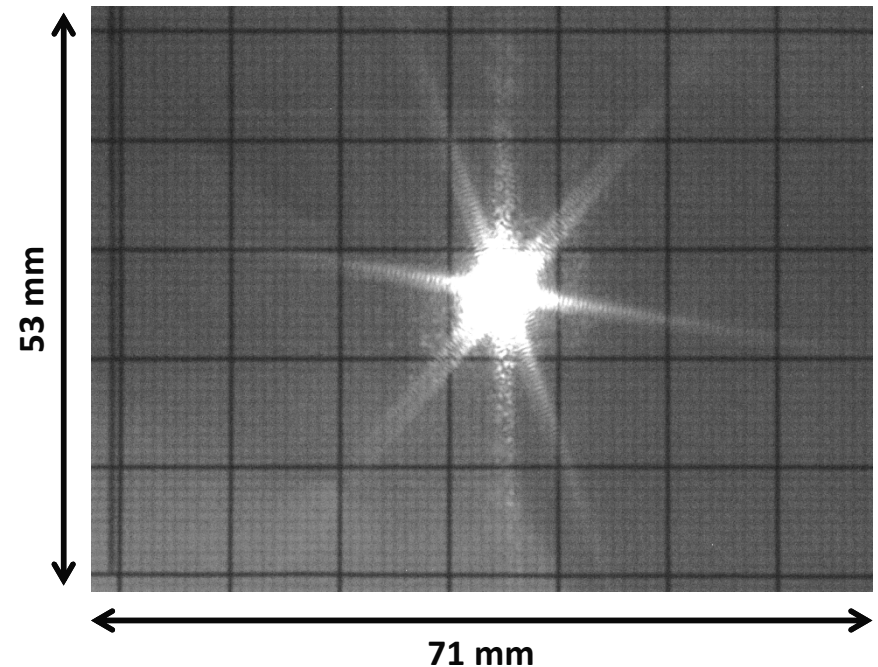
FIG. 2 — Solar image produced by a ray which is reflected by the paraboloid with the angle β .







- Read pixel intensities from CCD after subtracting representative “dark frame”
- Convert using black body calibration from *counts/μs* to W/m^2nm at 980 nm
- Account for reflectivity of pseudo-Lambertian surface
- Convert from W/m^2nm to # of Suns
 - Weight against filter band pass
 - Use ASTM G173 data to scale 980 nm values with the full spectrum
 - Multiply by ASTM G173 standard insolation to get pixel reading in W/m^2
- Compare to locally measured insolation to get map of concentration ratios



Sony ICX445 CCD - 1.2 MP
16-bit mono output format
Images captured at 640 x 480

Solar Thermal w/o Energy Storage	Chemical Thrusters	Electric Propulsion
<ul style="list-style-type: none"> Eliminated PCM and TPV Reduced solar collector size Added photovoltaic panels and batteries Used NASA year 2020 specific power projections for PV 	<ul style="list-style-type: none"> Astrium Hydrazine Monoprop Commercially available 1 N and 20 N models Isp: 220-230 s Removed thermal energy collection and storage system Added photovoltaic panels and batteries Used NASA year 2020 specific power projections for PV 	<ul style="list-style-type: none"> XHT-100 Hall Effect Thruster 95 W power draw Isp: 750-1000 s 3 – 10 mN Thrust Removed thermal energy collection and storage system Added photovoltaic panels and batteries Used NASA year 2020 specific power projections for PV

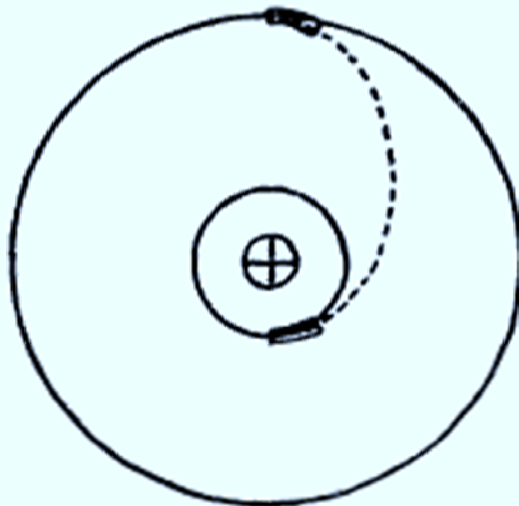
Identical Mass Fractions ($m_{\text{Propulsion \& Power}} = 58\%$)

Total ΔV and Delivery Time are Primary Comparison Metrics

TWO IMPULSE

ONE PERIGEE BURN
ONE APOGEE BURN

$T/W > 0.01$



LEO TO GEO

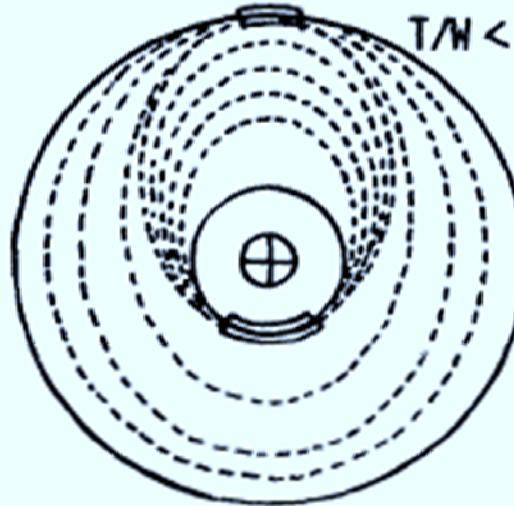
$14000 \leq \Delta V \leq 17000$ FPS

TRIP TIME < DAY

MULTI IMPULSE

MORE THAN ONE PERIGEE
BURNS AND MORE THAN
ONE "INSERTION" BURNS
NEAR FINAL APOGEE

$T/W < 0.1$



LEO TO GEO

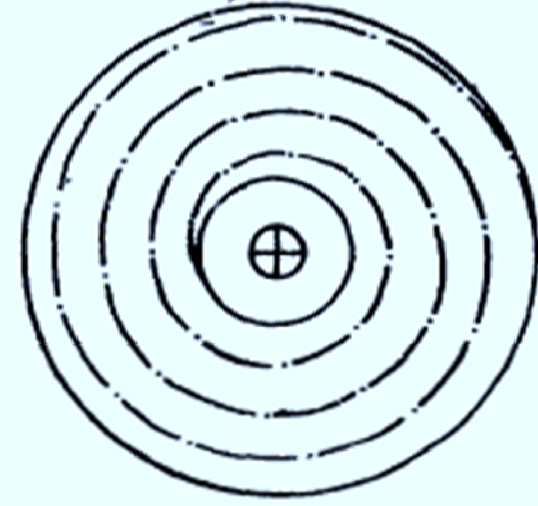
$14000 \leq \Delta V \leq 19200$ FPS

TRIP TIME > DAYS

CONTINUOUS BURN

SPIRAL TRAJECTORY

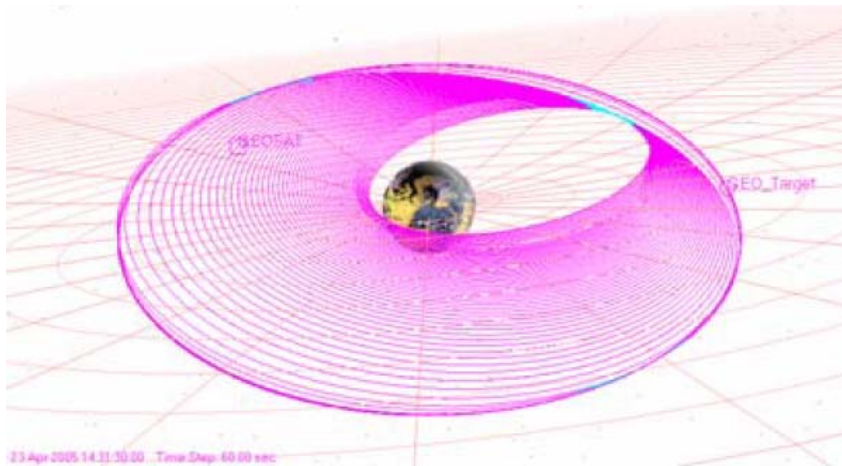
$T/W < 0.001$



LEO TO GEO

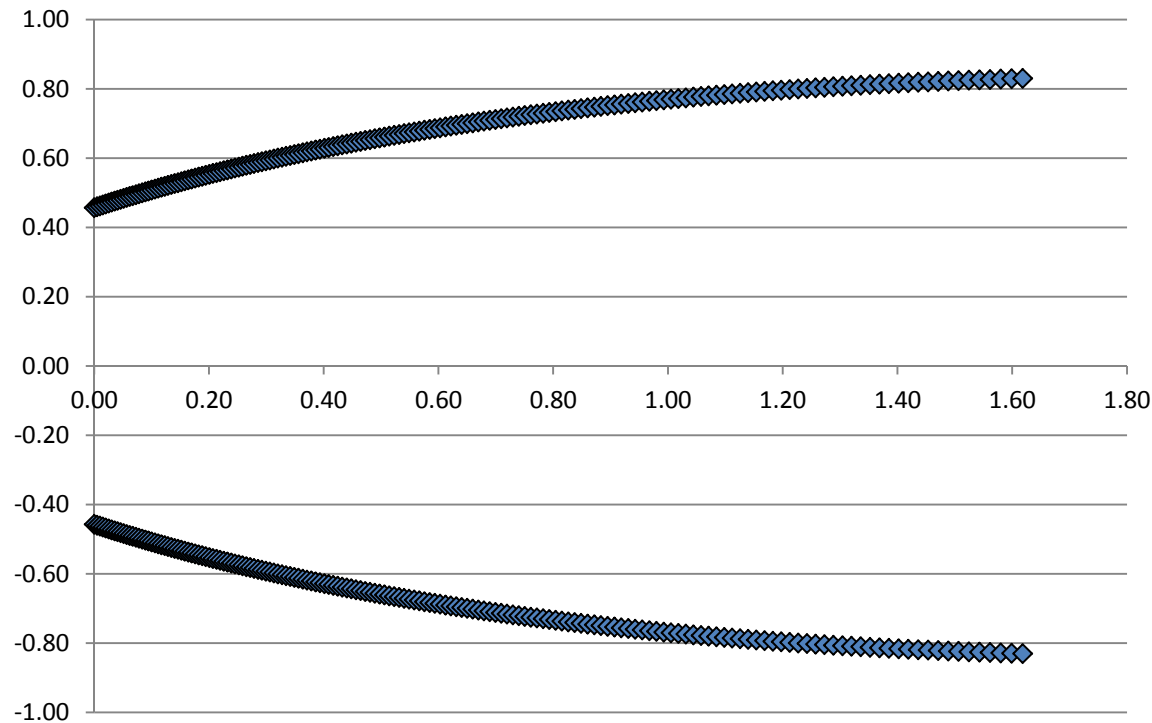
$\Delta V \approx 19200$ FPS

TRIP TIME > WEEK



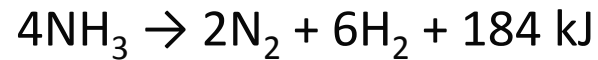
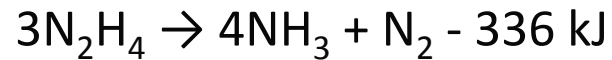
- 10% “On Time”
- 100 kg satellite
- Launch from Ariane 5 into GTO (350 x 35,717 km - 7°)
- Transfer to 0° at 116 °E
- Assumes ½ N thrust and 400 s I_{sp}
- 48 kg for *JUST* solar thermal engine and propellant

Start Date	1 April 2005, 00:00:00.00 (Julian Date 2453461.5)
End Date	6 May 2005, 09:11:16.96 (JD 2453496.88)
Elapsed Time	35 days, 9 hrs., 11 min.
Number of Maneuvers	58 (51 apogee kicks, 7 plane changes at node crossings). Two-orbit “hold” of 42 hrs., 20 min. introduced after apogee kick 48 to attain proper orbital phasing at GEO
Total Velocity Change	1,761 m/s
Propellant Consumption	36.184 kg
Final Mass	63.816 kg
Engine “On-Time”	80 hrs., 33 min.



- Defined by parametric equations given by *Welford and Winston 1978*
- **CAN NOT** be used to increase power due to low f/d ratio for the concentrator
- **CAN** be used to increase concentration ratio

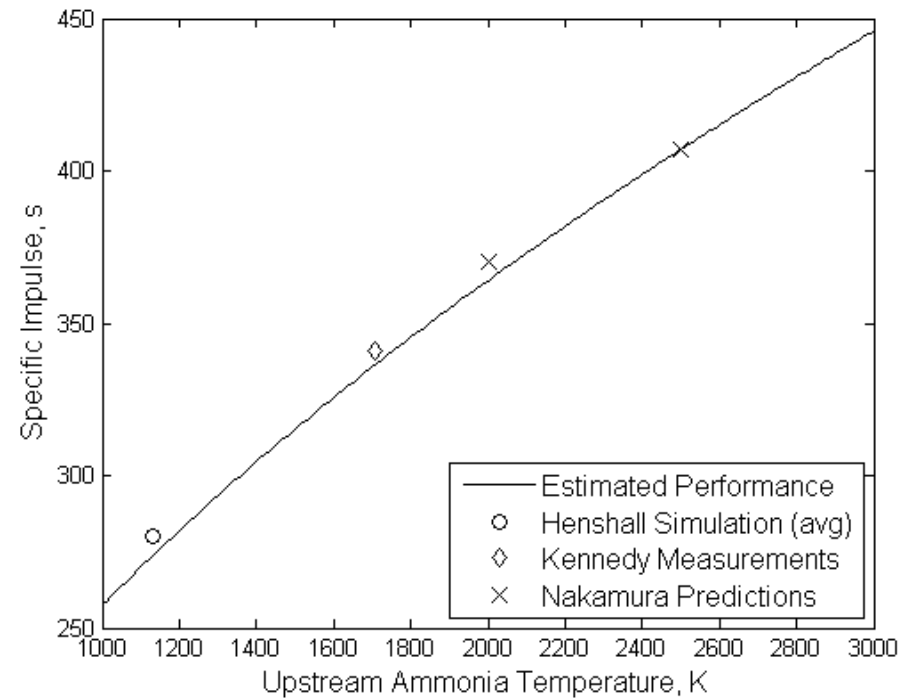
Diameter	Max Angle	Minimum Diameter	% Area Increase	Max Ratio	Minimum Spot	Spot Change	C Ratio Change
70	33.0	1.66	0%	3.24	0.914	0.84	5%
75	35.162	1.81	15%	2.99	1.046	1.09	-16%
80	37.7	2.09	32%	2.67	1.220	1.49	-29%



Net 1.6 MJ/kg

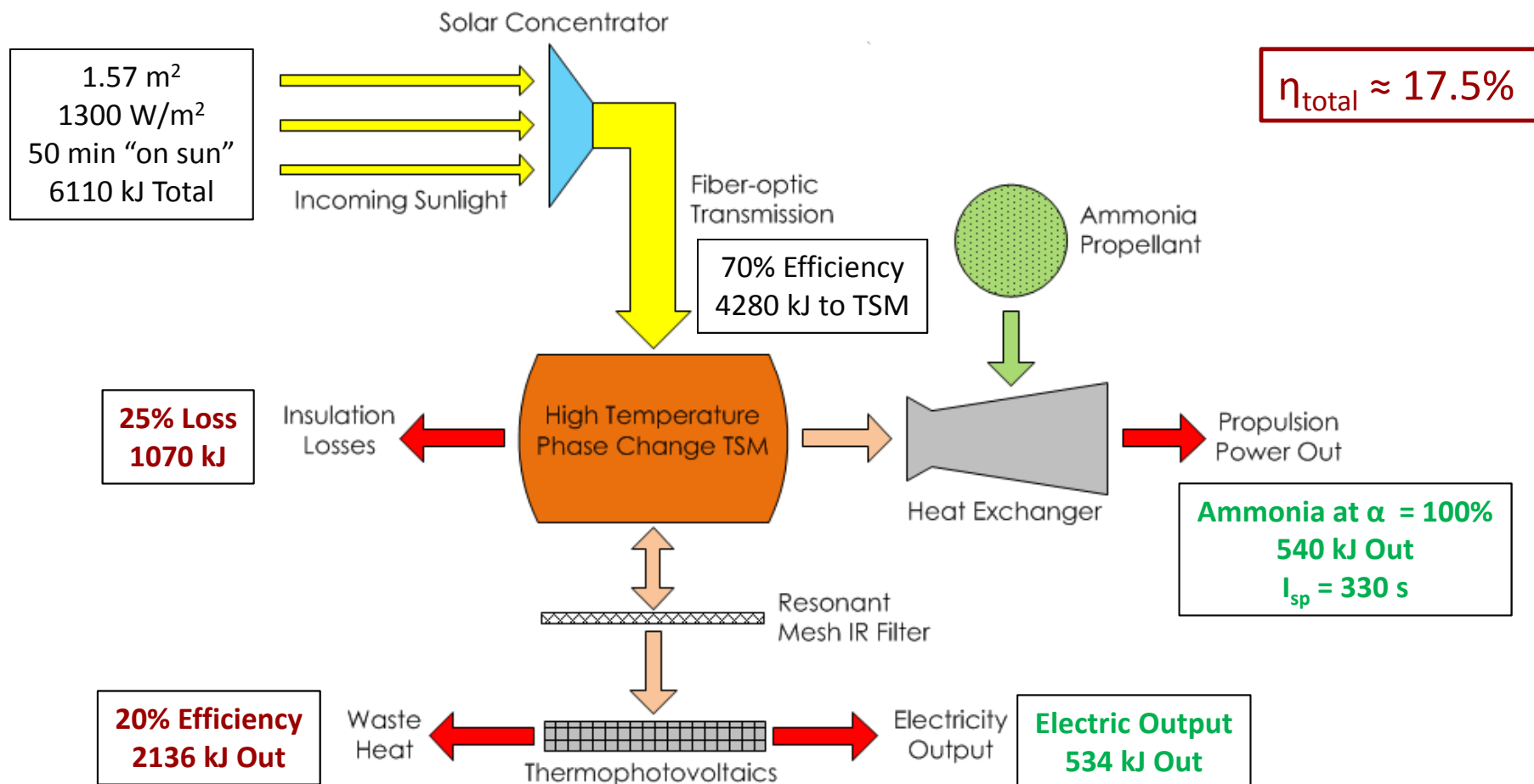
α_D	Isp
0	253
0.2	274
0.4	289
0.8	312
1	322

- Incomplete dissociation will lower performance
- Equilibrium calculations for 1500 K solar thermal thruster (*Colonna et. al. 2005*)
- Note, hydrazine thrusters typically have $\alpha_D \approx 55\%$



$$V_e = I_{sp} g_o = \sqrt{\frac{T_o R}{M} \frac{2\gamma}{\gamma - 1} \left[1 - \left(\frac{p_e}{p_o} \right)^{\frac{(\gamma-1)}{\gamma}} \right]}$$

For each 200 km Orbit





- Satellite is sized for a 200 km circular orbit
 - Storage sized for approx. 36 min eclipse
- Assumes 20% total electrical system efficiency
- Assumes 70% thermal collection efficiency
- Approximates impulsive burn profile with a 5% firing rule